AD-A110 689 CALIFORNIA UNIV RIVERSIDE DEPT OF PHYSICS F/G 20/8
CALCULATION OF ELECTRON-HYDROGEN, DEUTERIUM AND OXYGEN MOLECULE--ETC(U)
JUN 81 R T POE, B H CHOI F33615-77-C-2011

UNCLASSIFIED AFWAL-TR-81-2051 NL

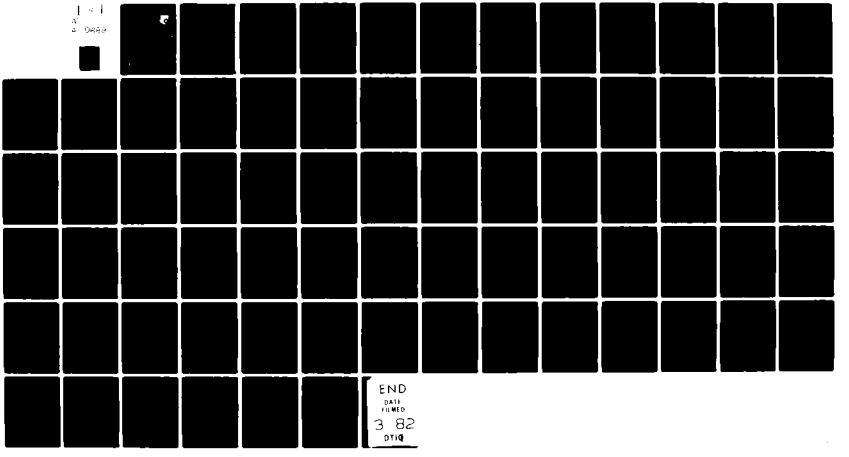

END
DATE FILMED
3 82
DTIC

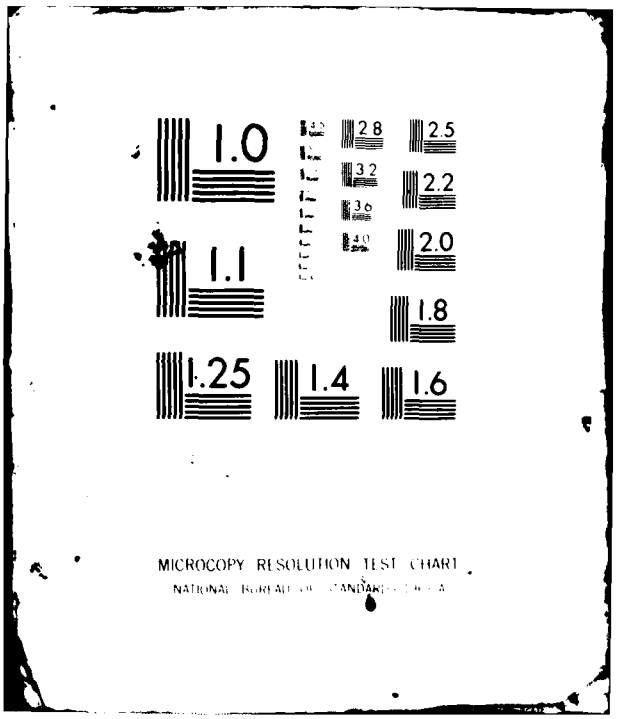
1.0
1.1
1.25
1.4
1.6
2.8
3.2
3.6
4.0
2.5
2.2
2.0
1.8
MICROCOPY RESOLUTION TEST CHART

LEVEL II

AFWAL-TR-81-2051

CALCULATION OF ELECTRON-HYDROGEN, DEUTERIUM AND OXYGEN MOLECULES

Professor R.T. Poe and Dr B.H. Choi

Department of Physics
University of California
Riverside CA 92521

June 1981

FINAL REPORT FOR PERIOD April 1979 - April 1980

Approved for public release; distribution unlimited

AERO PROPULSION LABORATORY
AIR FORCE WRIGHT AERONAUTICAL LABORATORIES
AIR FORCE SYSTEMS COMMAND
WRIGHT-PATTERSON AIR FORCE BASE, OHIO 45433

NOTICE

When Government drawings, specifications, or other data are used for any purpose other than in connection with a definitely related Government procurement operation, the United States Government thereby incurs no responsibility nor any obligation whatsoever; and the fact that the government may have formulated, furnished, or in any way supplied the said drawings, specifications, or other data, is not to be regarded by implication or otherwise as in any manner licensing the holder or any other person or corporation, or conveying any rights or permission to manufacture, use, or sell any patented invention that may in any way be related thereto.

This report has been reviewed by the Office of Public Affairs (ASD/PA) and is releasable to the National Technical Information Service (NTIS). At NTIS, it will be available to the general public, including foreign nations.

This technical report has been reviewed and is approved for publication.

PROJECT ENGINEER

ROBERT R. BARTHELEMY
Chief, Energy Conversion Branch

FOR THE COMMANDER

JAMES D. REAMS
Chief, Aerospace Power Division
Aero Propulsion Laboratory

"If your address has changed, if you wish to be removed from our mailing list, or if the addressee is no longer employed by your organization please notify AFWAL/POOC-3 , W-PAFB, OH 45433 to help us maintain a current mailing list."

Copies of this report should not be returned unless return is required by security considerations, contractual obligations, or notice on a specific document.

AIR FORCE/56780/22 December 1981 — 170

SECURITY CLASSIFICATION OF THIS PAGE (When Data Entered)

REPORT DOCUMENTATION PAGE	READ INSTRUCTIONS BEFORE COMPLETING FORM
1. REPORT NUMBER: AFWAL-TR-81-2051	2. GOVT ACCESSION NO.: AD-A110689
3. RECIPIENT'S CATALOG NUMBER	
4. TITLE (and Subtitle): Calculation of Electron-Hydrogen, Deuterium and Oxygen Molecules	5. TYPE OF REPORT & PERIOD COVERED: Final Apr 79 - Apr 80
	6. PERFORMING ORG. REPORT NUMBER
7. AUTHOR(s): Professor R.T. Poe Dr B.H. Choi	8. CONTRACT OR GRANT NUMBER(s): F33615-77-C-2011
9. PERFORMING ORGANIZATION NAME AND ADDRESS: Department of Physics, University of California, Riverside	10. PROGRAM ELEMENT, PROJECT, TASK AREA & WORK UNIT NUMBERS: 2301S203
11. CONTROLLING OFFICE NAME AND ADDRESS: Energy Conversion Branch, Aerospace Power Division Aero Propulsion Laboratory, AFWAL/POOC Wright-Patterson AFB OH 45433	12. REPORT DATE: June 1981 13. NUMBER OF PAGES: 70
14. MONITORING AGENCY NAME & ADDRESS (if different from Controlling Office)	15. SECURITY CLASS. (of this report): Unclassified 15a. DECLASSIFICATION/DOWNGRADING SCHEDULE

16. DISTRIBUTION STATEMENT (of this Report)

Approved for public release; distribution unlimited

17. DISTRIBUTION STATEMENT (of the abstract entered in Block 20, if different from Report)

18. SUPPLEMENTARY NOTES

19. KEY WORDS (Continue on reverse side if necessary and identify by block number)

Electron-Hydrogen, Deuterium and Oxygen Mol[illegible] Scattering

Vibrational Transition Cross Section

Elastic Scattering Cross Section

Rotational and Vibrational Adiabatic Nuclei Approximation

20. ABSTRACT (Continue on reverse side if necessary and identify by block number)

Calculations are made on the vibrational transition cross sections of e-H_2, D_2 scatterings in the energy range of $0 \sim 10$eV. Both hybrid theory and the simultaneous vibrational and rotational adiabatic-nuclei approximation are employed in the calculation. It turns out that the latter approximation scheme yields better results than the hybrid theory approach when compared with experimental measurements on $0 \rightarrow v$ vibrational excitation. The resonance peaks of the elastic scattering and vibrational excitation cross section obtained from the vibrational and rotational adiabatic-nuclei approximation are

DD FORM 1 JAN 73 1473 EDITION OF 1 NOV 65 IS OBSOLETE

SECURITY CLASSIFICATION OF THIS PAGE (When Data Entered)

quite broad between $2 \sim 3$ eV, which are in good agreements with experimental data. This seems to indicate that the periods of the vibrational and rotational motions are comparable to each other and longer than the lifetime of the compound molecule. In general, the rate of the vibrational transition decreases as the quantum number change increases. The $e\text{-}O_2$ vibrational transition cross sections have also been explored with a semi-quantitative analysis.

FOREWORD

This report describes an effort conducted by personnel of the Department of Physics, University of California, Riverside, under Contract F33615-77-C-2011, Project 2301.

The work reported herein was performed during the period 15 April 1979 to 15 April 1980, under the direction of the authors, Dr. Robert T. Poe, Principal Investigator, and Dr. B. H. Choi, Co-Investigator. The report was released by the authors in October 1980.

The authors wish to thank Dr. Alan Garscadden for his valuable discussions. The authors wish to thank Dr. James C. Sun, Mrs. Glenna Paschal and Mrs. Susan Miles for their assistance in preparing this report.

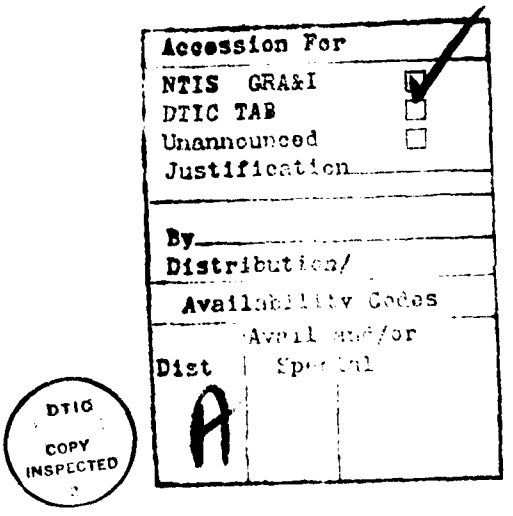

TABLE OF CONTENTS

LIST OF ILLUSTRATIONS

LIST OF TABLES

SECTION I

INTRODUCTION

In the broad class of electron-molecule collision systems, the electron-hydrogen (or deuterium) molecule scattering represents the most basic prototype. The fundamental importance in the study and understanding of this system has indeed been responsible for the considerable theoretical activities in recent years.

Lane and Geltman (Ref. 1) performed a semi-empirical, rotational close-coupling calculation to obtain the rotational excitation and the pure elastic scattering cross sections. This calculation is semi-empirical in the sense that the interaction potential employed contains some adjustable parameters in addition to the conventional cutoff radius of the polarization potential. Henry and Lane (Ref. 2) carried out the rotational close-coupling calculations where both the exchange and the polarization potentials, the latter computed in Lane and Henry (Ref. 3), are included.

Using the fixed nuclei approximation with two-center approach, Hara (Ref. 4) calculated the e-H_2 elastic cross sections. Temkin and Vasavada (Ref. 5) and Temkin, Vasavada, Chang and Silver (Ref. 6) performed calculation again within the fixed-nuclei approximation, but with the single center expansion of the potential and the electronic wave function distorted by the polarized orbital method. Temkin and Faisal

(Ref. 7), and Chang and Temkin (Ref. 8) obtained the rotational excitation cross sections using the rotationally adiabatic nuclei approximation. Henry and Chang (Ref. 9) performed e-H_2 scattering calculation employing the frame transformation theory.

Most of these calculations have been confined to either pure elastic, vibrationally elastic scattering, or the rotational excitation within the ground vibrational manifold. These approaches are not appropriate for the general calculation of the electron-molecule vibrational transition scattering cross sections. On the other hand, the rigorous simultaneous vibrational and rotational close-coupling scheme, resulting in large dimensions of the coupled differential equations, is still computationally impracticable at the present.

The hybrid theory approach, initiated by Temkin and reformulated by Choi and Poe , was a logical choice for the study of e-H_2 and e-D_2 vibrational transition scatterings. In this formulation, the rotational degrees of freedom is treated within the framework of adiabatic nuclei approximation while the vibrational degrees of freedom is dynamically (close) coupled in the scattering equation. Physically, the hybrid theory in essence recognizes the difference between the slow moving rotation of the molecule during the scattering process and the much faster molecular vibrations. The hybrid theory was successfully applied to the e-N_2 case and to a detailed

study of the e-CO scatterings ; the latter was under the auspices of APL-WPAFB and formed the impetus for this research.

In the present study, two different theoretical approaches were employed. In contrast to the success in e-N_2 and e-CO cases, the hybrid theory approach yields results grossly incompatible with experiments. The second approach, the simultaneous vibrational and rotational adiabatic nuclei approximation, yields results in much better agreement with available data; and the calculational results from this approach on the vibrationally elastic and vibrational transition cross sections, and the rate coefficients of the transitions are systematically reported.

In Section II, the procedure of our theoretical calculation are presented, with regard to both the input interaction potentials between the incident electron and the target molecule, and the dynamic scattering approaches used. The results are presented in Section III. Discussions and Conclusions are given in Section IV, including a brief report on our qualitative study on the e-O_2 scattering problem.

SECTION II

THE PROCEDURES OF COMPUTATION

1. Input Potential

The computational procedures of e-H_2, D_2 interaction potential are basically similar to the previous e-CO case. The potential is written as

$$V = V^{(stat)}(r,R,\gamma) + V^{(pol)}(r,R,\gamma) + V^{(ex)}(r,R,\gamma) \qquad (1)$$

The static interaction potential is the sum of Coulomb interactions between the incident electron and the electronic clouds of H_2 or D_2 in the ground state, and between the electron and nuclei. It is again evaluated through the following harmonic expansion

$$V^{(stat)}(r,R,\gamma) = \sum_{\lambda} V_{\lambda}^{(stat)}(r,R) P_{\lambda}(\cos\gamma) \qquad (2)$$

For the present homonuclear target molecule cases, only λ=even terms contribute to the summation given by Eq. (2).

The molecular wave functions of H_2 and D_2 of the ground electronic state, which were used for generating static interaction potential, are those obtained by Das and Wahl (Ref. 10). They performed extended self-consistent field calculations with "Optimized Valence Configuration" scheme. The wave functions were obtained in the following form

$$\Psi_e = A1\sigma_g^2 + B1\sigma_u^2 + C1\pi_u^2 + D2\sigma_g^2 + E1\pi_g^2 + F3\sigma_g^2 \qquad (3)$$

Here, the major configuration for the ground electronic state of

H_2, D_2 is $1\sigma_g^2$ and A,B,C,... are the configuration mixing coefficients. For the close-coupling calculations of the vibrational transitions, we have evaluated the static potential for the internuclear separations R=1.0, 1.2, 1.3, 1.4, 1.5, 1.6, 1.8, 2.0 and 3.0 a_o for which the molecular wave functions of Eq. (3) were given in Ref. 10. Some harmonic components of the potential are shown in Figure 1 at the equilibrium internuclear separation R_o=1.4 a_o. The sharp kinks, which are the lowest points of the potential, corresponds to the center of hydrogen or deuteron nuclei. All potentials are basically attractive. In Figure 2, the variation of the harmonic components are illustrated as functions of the internuclear separations R. As R decreases, the potentials become more attractive.

The dominant contribution of the long range part of the static potential arises from the quadrupole moments of H_2 (or D_2) as follows,

$$V_2(r,R) \underset{r\to\infty}{\sim} \frac{Q(R)}{r^3} \tag{4}$$

We obtained $Q(R_o)$ = 0.457 a.u. from the above ab initio wave functions.

In Eq. (1), the $V^{(pol)}(r,R,\gamma)$ is the polarization potential due to the induced polarizabilities of target in the presence of incident electron given by

$$V^{(pol)}(r,R,\gamma) = -\frac{1}{2r^4}[\alpha_o(R)+\alpha_2(R)P_2(\cos\gamma)] \times \{1-\exp[-(r/r_c(R))^6]\} \tag{5}$$

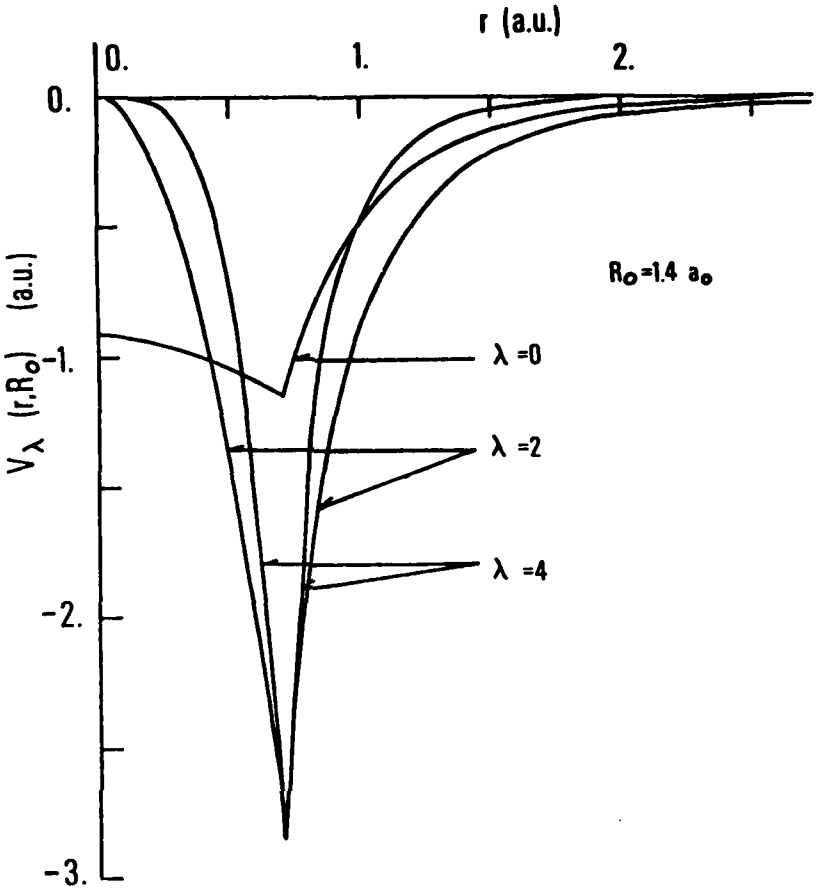

Figure 1. The Harmonic Components of Static Potential at the Equilibrium Distance of H_2.

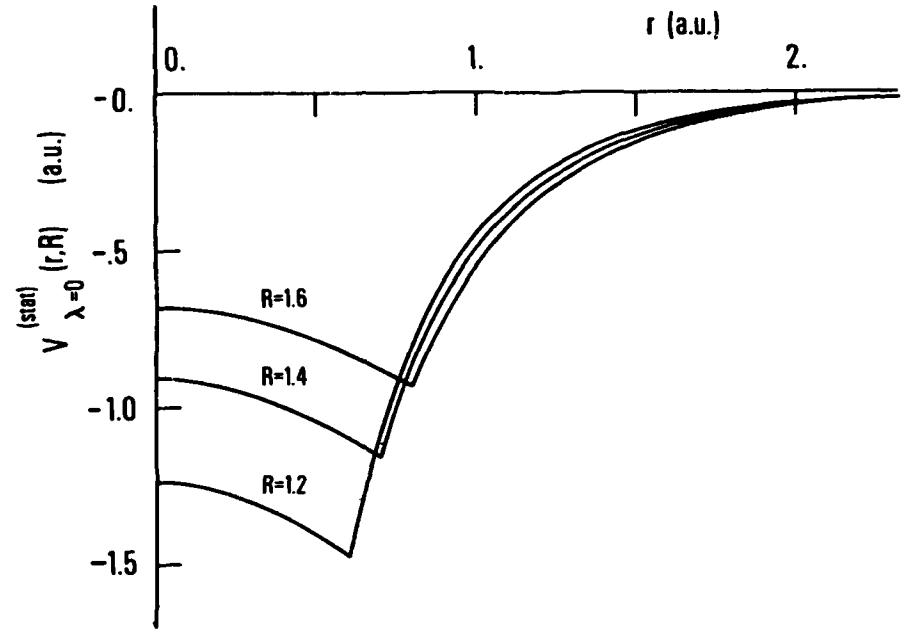

(a) $\lambda = 0$

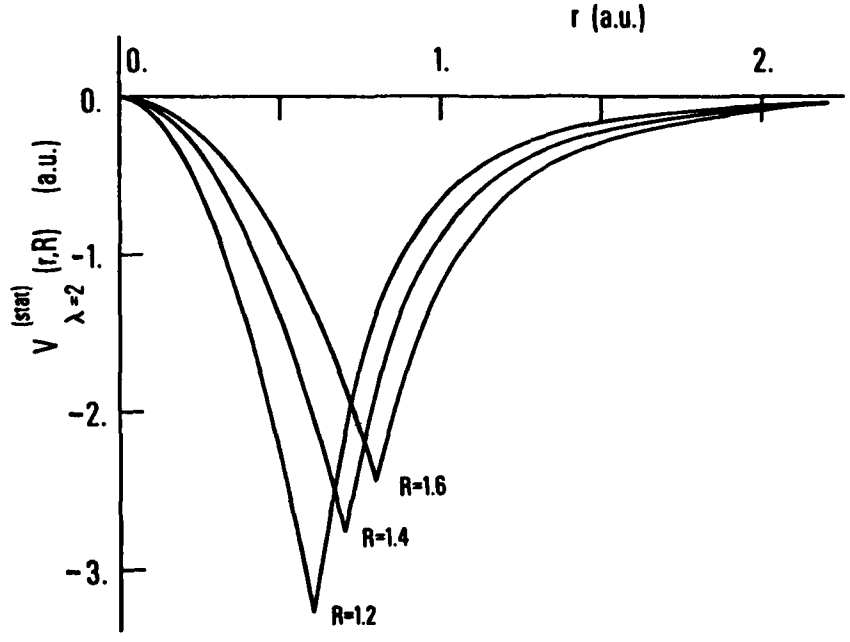

(b) $\lambda = 2$

Figure 2. Variation of Static Potential as Functions of the Internuclear Separations.

The $\alpha_o(R)$ and $\alpha_2(R)$ are the spherical and nonspherical polarizabilities, respectively. For the present H_2 and D_2 molecules, Kolos and Wolniewicz (Ref. 11) obtained quite accurate parallel and perpendicular polarizabilities, $\alpha_{||}(R)$ and $\alpha_{\perp}(R)$, with a variation perturbation method. We have used these values for computing polarizabilities through the equations,

$$\alpha_o(R) = \frac{1}{3}(\alpha_{||}(R)+2\alpha_{\perp}(R))$$
$$\alpha_2(R) = \frac{2}{3}(\alpha_{||}(R)-\alpha_{\perp}(R)) \qquad (6)$$

In Eq. (5), the $r_c(R)$ is the cutoff radius which is roughly given by the boundary of the electronic coulds of target molecules H_2 and D_2. Here, we have explicitly taken into account the dependence on the internuclear separation, R for the radius, in contrast to the previous e-CO case. The reason is that the stretching of the internuclear separation due to the vibrational motion is considerably large for the H_2 and D_2 molecule, whereas it is small for the CO molecule. Thus, the R dependence of the cutoff radius is minor for CO. The empirical method of determining the radius at each R will be subsequently discussed.

The treatment of full non-local exchange potential for the present calculation of the vibrational transition cross section is again an unmanageably complex task. Thus, the exchange effects have been treated with the local exchange potential $V^{(ex)}(r,R,\gamma)$ in Eq. (1). It is essentially the same form as used in the previous e-CO scattering study and given as follows:

$$V^{(ex)}(r,R,\gamma) = -\frac{2}{\pi}k_F(r,R,\gamma)F(\eta) \tag{7}$$

with

$$F(\eta) = \frac{1}{2} + \frac{1-\eta^2}{4\eta}\log\left|\frac{1+\eta}{1-\eta}\right|$$

$$k_F(r,R,\gamma) = (3\pi^2\rho(r,R,\gamma))^{1/3}$$

$$\eta = \eta(r,R,\gamma) \tag{8}$$

$$= k(r,R,\gamma)/k_F(r,R,\gamma)$$

$$k(r,R,\gamma) = [2(E+I(R)) + k_F^2(r,r,\gamma)]^{1/2}$$

Here, $\rho(r,R,\gamma)$ is the electronic density of target molecule H_2 or D_2. The I(R) is the ionization potential of target molecule as a function of the internuclear separation R. These potentials were computed from

$$I(R) = E_{H_2^+}(R) - E_{H_2}(R) \tag{9}$$

The $E_{H_2^+}$ and $E_{H_2}(R)$ are the energy curves of the ground electronic states of the molecules H_2^+ and H_2, respectively. The energy curves obtained by Hunter, Gray, and Pritchard (Ref.12), and Kolos and Wolniewicz (Ref. 13) for those molecules were used to evaluate the ionization potential. The result is slightly bigger than the experimental one at the equilibrium separation $R_o = 1.4\ a_o$. Thus, we have renormalized the theoretical values based on this experimental ionization potential at $R_o = 1.4\ a_o$. The final theoretical results are tabulated in Table 1.

TABLE 1

THE IONIZATION POTENTIAL OF $H_2(D_2)$ AS FUNCTION OF THE INTER-NUCLEAR SEPARATION

R	1.0	1.2	1.3	1.4	1.5	1.6	1.7	1.8	1.9
I	0.624	0.592	0.577	0.564	0.552	0.541	0.521	0.504	0.459

The entries of the above table are in atomic units. For the present homonuclear target molecules,

$$\rho(r,R,\gamma) = \rho(r,R,\pi-\gamma) \tag{10}$$

Thus, the exchange potential is expanded in terms of the even harmonic components as

$$V^{(ex)}(r,R,\gamma) = \sum_{\lambda=even} V_\lambda^{(ex)}(r,R)P_\lambda(\cos\gamma) \tag{11}$$

The same remark was also applied to the static potential $V^{(stat)}(r,R,\gamma)$.

2. Dynamic Calculations

A. Hybrid Tneory Approach:

We have computed e-H_2,D_2 vibrational transition cross sections employing the hybrid theory. Here the method of the vibrational close-coupling calculations is similar to that of the e-CO case previously reported , except that the computer program we made should be modified appropriately for the present homonuclear target molecule. To obtain the cutoff radius r_c, vibrationally elastic scattering calculations were performed with v_{max}=1. Here, v_{max} is the number of the vibrational

states included in the close-coupling scheme. The r_c was determined such that the vibrational elastic resonance peak of σ_u scattering wave occur around 2∿3 eV of the incident energy. After r_c was obtained, we have carried out the still considerably complicated the vibrational close-coupling calculations with v_{max}=1,2,3,4,5.

It turns out that the convergence of the vibrational elastic and excitation cross sections on the basis (vibrational) states is very slow. Furthermore, sharp peak and substructure appear in the cross sections. Sample results of the hybrid theory calculation for e-H_2 scattering are shown in Figure 3(a) and (b) for vibrationally elastic (0→0) and (0→1) excitation cross sections, respectively, with v_{max}=1,2,3.

As v_{max} increases, the sharp peak and the substructure tend to be more pronounced. This is in contrast to the experimental measurements which yield broad resonance in both the elastic and the vibrational excitation cross sections. No substructures of the cross sections appear in the experimental ones. Therefore, the hybrid theory where the rotational motions of target molecules are neglected and the vibrational motions are treated dynamically seems to be inappropriate for the present e-H_2, D_2 cases. A computational scheme which treats the rotational and vibrational motions with <u>equal</u> degrees of approximations could be suited for the electron-light molecule scattering.

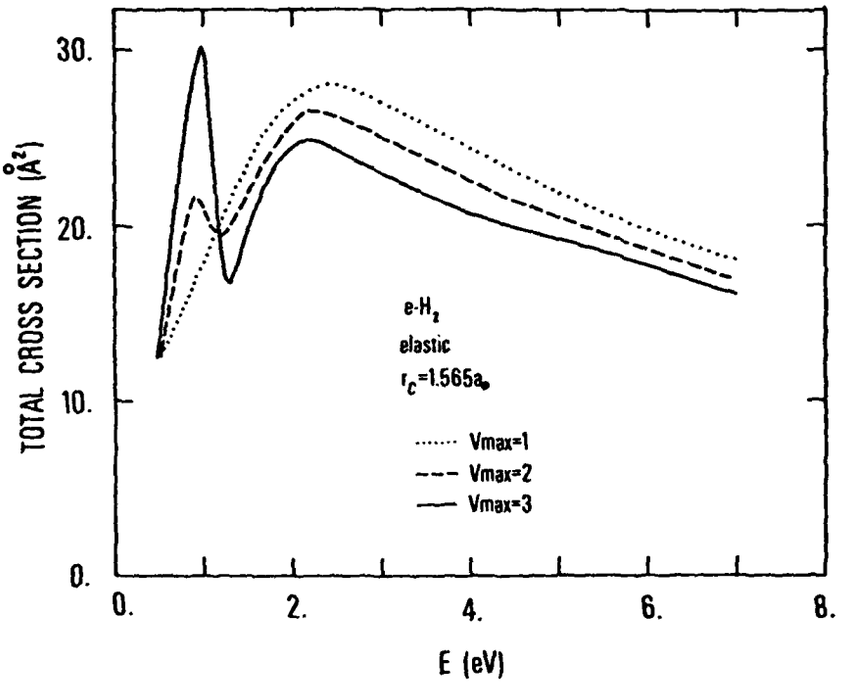

(a) Elastic Scattering

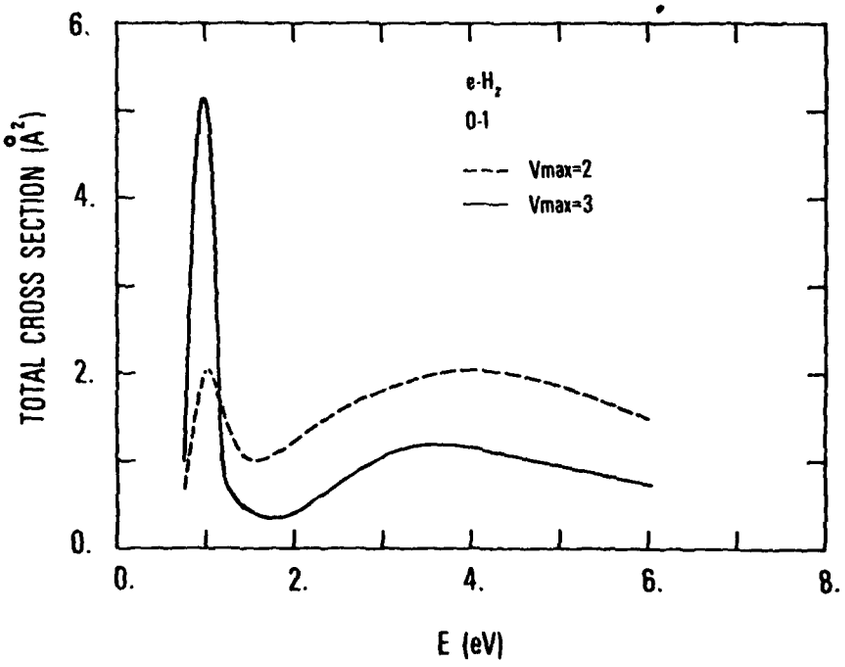

(b) 0 → 1 Vibrational Excitation

Figure 3. The Hybrid Theory Calculations of e-H_2 Collisions.

B. Simultaneous rotational and vibrational adiabatic approximation.

In this approach, the transition matrix elements $T^{(m')}_{\ell',\ell}(T)$ are obtained by solving the following coupled differential equation.

$$\left[\frac{d^2}{dr^2} - \frac{\ell'(\ell'+1)}{r^2} + k^2\right] g^{(m')}_{\ell',\ell}(R,r)$$

$$= \frac{2\mu_e}{h^2} \sum_{\ell''} V^{(m')}_{\ell',\ell''}(R,r)\, g^{(m')}_{\ell'',\ell}(R,r) \tag{12}$$

with the asymptotic boundary condition

$$g^{(m')}_{\ell',\ell}(R,r) \underset{r\to\infty}{\sim}$$

$$i^{\ell'}\{\delta_{\ell',\ell}F_{\ell'}(kr) + T^{(m')}_{\ell',\ell}(R)\,(G_{\ell'}(kr)+iF_{\ell'}(kr))\} \tag{13}$$

Here, $k^2 = 2\mu_e E/h^2$ with E the incident energy when the target molecule is in the ground vibrational state and

$$V^{(m')}_{\ell',\ell''}(R,r) = (-1)^{m'} \sum_{\lambda} \frac{1}{2\lambda+1}[(2\ell'+1)(2\ell''+1)]^{1/2} \langle \ell' o \ell'' o | \lambda o\rangle$$

$$x \langle \ell' m' \ell'' -m' | \lambda o\rangle V_\lambda(r,R) \tag{14}$$

$$F_{\ell'}(x) = x j_{\ell'}(x)$$

$$G_{\ell'}(x) = -x n_{\ell'}(x) \tag{15}$$

The $V_\lambda(r,R)$ is the λth harmonic component of $V(r,R,\gamma)$ given by Eq. (1). Other notations are the same as in the previous report of e-CO scattering. The matrix elements $T^{(m')}_{\ell',\ell}(R)$ thus obtained are basically those of elastic scattering with the fixed-nuclei approximation at each internuclear separation R. The vibrational transition matrix elements $T^{(m')}_{\ell'v',\ell v}$ are computed from these elements $T^{(m')}_{\ell',\ell}(R)$ employing the following vibrational adiabatic procedure

$$T^{(m')}_{\ell'v',\ell v} = \int R^2 dR \phi_{v'}(R) T^{(m')}_{\ell',\ell}(R) \phi_v(R) \tag{16}$$

Here, $\phi_v(R)$ is the vibrational wave functions of the target molecule. With $T^{(m')}_{\ell'v',\ell v}$'s obtained from Eq. (16), the differential and integral vibrational transition cross sections are computed from

$$\frac{d\sigma_{v\to v'}}{d\Omega}(\theta) = \frac{4\pi}{k_v^2} \sum_{\lambda\mu} \frac{1}{2\lambda+1} \Big| \sum_{\ell'\ell m'} (-1)^{m'} (2\ell+1)^{1/2} \langle \ell'\mu\ell 0 | \lambda\mu \rangle$$

$$\times \langle \ell' m' \ell -m' | \lambda 0 \rangle \, T^{(m')}_{\ell'v',\ell v} Y_{\ell'\mu}(\theta,\phi) \Big|^2 \tag{17}$$

$$\sigma_{v\to v'} = \frac{4\pi}{k_v^2} \sum_{\ell'\ell m'} \left| T^{(m')}_{\ell'v',\ell v} \right|^2 \tag{18}$$

As in the hybrid theory presented in the Ref. 14 and the previous report, the cross sections of the simultaneous vib-rotational transitions $(vjm_j)\to(v'j'm'_j)$ are obtained employing the rotationally adiabatic-nuclei approach. Thus, the differential and the integral cross sections of those transitions are computed from

$$\frac{d\sigma_{vj\to v'j'}}{d\Omega}(\theta) = \frac{4\pi}{k_v^2(2j+1)} \sum_{m_j m_j'} \Big| \sum_{J\ell'\ell} (2\ell+1)^{1/2}$$

$$\times \langle \ell' m_j - m_j' \; j' m_j' \,|Jm_j\rangle \langle \ell o j m_j | Jm_j\rangle T^J_{v'j'\ell',vj\ell}$$

$$\times Y_{\ell' m_j - m_j'}(\theta,\phi)\Big|^2 \tag{19}$$

$$\sigma_{vj\to v'j'} = \frac{4\pi}{k_v^2(2j+1)} \sum_{\ell\ell'J} (2J+1) \left| T^J_{v'j'\ell',vj\ell} \right|^2 \tag{20}$$

with

$$T^J_{v'j'\ell',vj\ell} = \frac{[(2j'+1)(2j+1)]^{1/2}}{2J+1} \sum_{m'} \langle \ell' m' j' 0 | Jm' \rangle$$

$$\times T^{(m')}_{\ell'v',\ell v} \langle \ell m' j o | Jm' \rangle \tag{21}$$

Here, $T^{(m')}_{\ell'v',\ell v}$'s are again given by Eq. (16).

The present scheme is in contrast to the hybrid theory approach where the vibrotational transition matrix elements $T^{(m')}_{\ell'v',\ell v}$ are directly obtained from the following dynamically coupled differential equation and corresponding asymptotic boundary condition,

$$\left[\frac{d^2}{dr^2} - \frac{\ell'(\ell'+1)}{r^2} + k_{v'}^2,\right] g^{(m')}_{\ell'v',\ell v}(r)$$

$$= \frac{2\mu_e}{h^2} \sum_{\ell'' v''} V^{(m')}_{\ell'v',\ell''v''}(r)\, g^{(m')}_{\ell''v'',\ell v}(r) \tag{22}$$

$$(\ell,\ell',\ell'' \geq |m'|)$$

and

$$g^{(m')}_{\ell'v',\ell v}(r) \underset{r\to\infty}{\sim}$$

$$i^{\ell'}\left(\frac{k_v}{k_{v'}}\right)^{1/2}\{\delta_{\ell'\ell}\delta_{v'v}F_{\ell'v'}(r) + T^{(m')}_{\ell'v',\ell v}(G_{\ell'v'}(r)+iF_{\ell'v'}(r))\} \tag{23}$$

Here, the notations are the same as in the previous report.

Since λ=even in the harmonic components of the potential, $(-1)^{\ell'} = (-1)^{\ell''}$ in Eq. (12). Thus, that coupled differential equation is solved with even ℓ's for "gerade" scattering waves and odd ℓ's for "ungerade" scattering waves. According to m'=0,1,2,..., we have σ_g, σ_u, π_g, π_u, ... scattering waves for which the coupled differential equation of Eq. (12) is solved separately. The number of the coupled channels is then given by

$$N_c^g = \text{no. of even } \ell\text{'s such that } m' \leq \ell \leq \ell_{max} \tag{24}$$

for "gerade" waves and

$$N_c^u = \text{no. of odd } \ell\text{'s such that } m' \leq \ell \leq \ell_{max} \tag{25}$$

for "ungerade" waves. We have chosen ℓ_{max} = 8 and thus the numbers of the coupled channels are 5, 4, 4, 4, ... for σ_g, σ_u, π_g, π_u, ... scattering waves, respectively. The coupled differential equation is integrated out from the origin up to 20 a_o where the potential is practically zero.

The cutoff radius' $r_c(R)$ of the polarization potential should roughly be given by the boundaries of the electronic cloud of target molecule at each internuclear separation R. With the incident electron being located beyond those boundaries, the polarization potential of Eq. (5) becomes effective. However, there exists no strict theoretical criteria for the precise values of these radius'. Thus, we have determined $r_c(R)$

in a semiempirical manner as before. In the present e-H_2, D_2 scattering, the broad resonance arises from $^2\Sigma_u$ compound state. This indicates that the σ_u scattering wave is the resonance wave in the present energy region (0→10 eV.). Therefore, we have carried out fixed-nuclei (elastic) close-coupling calculation for the resonance (σ_u) wave and chosen the value of $r_c(R)$ such that the broad resonance peaks occur between 2∿3 eV at each internuclear separation R. The results are tabulated in TABLE 2.

TABLE 2

CUTOFF RADIUS OF THE POLARIZATION POTENTIAL AS FUNCTION OF INTERNUCLEAR SEPARATION

R	1.0	1.2	1.3	1.4	1.5	1.6	1.8	2.0
r_c	1.022	1.235	1.365	1.5	1.697	1.901	2.381	2.91

The entries of the above table are in atomic units (a_o). The H_2 and D_2 vibrational wave functions computed from Hulbert-Hirschfelder energy curve (Ref. 15) were employed to generate the vibrational transition matrix elements $T^{(m')}_{\ell'v',\ell v}$ given by Eq. (16).

SECTION III

RESULTS OF CALCULATION AND COMPARISON WITH EXPERIMENTAL DATA

We have computed the integral, differential and momentum transfer cross section for the vibrationally elastic and inelastic scattering of H_2,D_2 up to 10 eV of energy.

In TABLE 3, e-H_2 integral cross sections are tabulated. The total energy E and the incident (kinetic) energy E_{inc} are in units of eV. The cross sections are in units of a.u. (a_o^2). The relation $E=E_{inc}+\varepsilon_{vi}$ is satisfied with ε_{vi} the initial vibrational energy level of H_2. The ε_o is set to zero. In the table, a±n should read as ax10$^{\pm n}$. The v_i and v_f are the initial and the final vibrational quantum numbers, respectively. The diagonal entries of the table are the vibrationally elastic cross sections ($v_i=v_f$). The upper diagonal and lower diagonal entries of the table are the vibrational excitation and deexcitation cross sections, respectively. It is seen from the table that the relation of detailed balance

$$k_v^2\sigma_{v\to v'} = k_{v'}^2\sigma_{v'\to v} \tag{26}$$

is satisfied. The above results are the sum of σ_g-, σ_u-, π_g-, π_u-, δ_g-, and δ_u- wave partial cross sections. The contributions of the higher scattering waves to the cross sections are found to be small. Furthermore, the major contribution to the vibrational transition and elastic cross sections in the broad resonance region (2~5 eV) arise from σ_u- wave.

TABLE 3

THE ELASTIC AND VIBRATIONAL TRANSITION CROSS SECTIONS OF ELECTRON-HYDROGEN MOLECULE SCATTERING

E = 0.75

E_{inc}	v_i \ v_f	0	1
0.75	0	0.5233+2	0.6174+0
0.2343	1	0.1976+1	0.5720+2

E = 1.0

E_{inc}	v_i \ v_f	0	1
1.0	0	0.6016+2	0.7249+0
0.4843	1	0.1496+1	0.6404+2

E = 1.25

E_{inc}	v_i \ v_f	0	1	2
1.25	0	0.6895+2	0.7902+0	0.3224-1
0.7343	1	0.1345+1	0.7165+2	0.9184+0
0.2479	2	0.1625+0	0.2720+1	0.7432+2

Table 3. The Elastic and Vibrational Transition Cross Sections of Electron-Hydrogen Molecule Scattering (Continued)

E = 1.5

E_{inc}	v_i \ v_f	0	1	2	3
1.5	0	0.7768+2	0.8913+0	0.5056-1	0.2291-2
0.9843	1	0.1358+1	0.7908+2	0.1109+1	0.5103-1
0.4979	2	0.1523+0	0.2193+1	0.8077+2	0.5428+0
0.0407	3	0.8436-1	0.1232+1	0.6633+1	0.8215+2

E = 1.75

E_{inc}	v_i \ v_f	0	1	2	3
1.75	0	0.8508+2	0.1045+1	0.7332-1	0.6846-2
1.2343	1	0.1482+1	0.8508+2	0.1276+1	0.1449+0
0.7479	2	0.1715+0	0.2105+1	0.8574+2	0.1154+1
0.2907	3	0.4120-1	0.6154+0	0.2970+1	0.8608+2

E = 2.0

E_{inc}	v_i \ v_f	0	1	2	3	4
2.0	0	0.9025+2	0.1222+1	0.9863-1	0.1133-1	0.5806-2
1.4843	1	0.1647+1	0.8887+2	0.1459+1	0.2135+0	0.2173-1
0.9979	2	0.1976+0	0.2170+1	0.8852+2	0.1395+1	0.2021+0
0.5407	3	0.4193-1	0.5860+0	0.2574+1	0.8799+2	0.9059+0
0.1132	4	0.1025+0	0.2849+0	0.1782+1	0.4327+1	0.8736+2

Table 3. The Elastic and Vibrational Transition Cross Sections of Electron-Hydrogen Molecule Scattering (Continued)

E = 2.25

E_{inc}	v_i \ v_f	0	1	2	3	4
2.25	0	0.9301+2	0.1380+1	0.1208+0	0.1658-1	0.1146-1
1.7343	1	0.1790+1	0.9041+2	0.1629+1	0.2694+0	0.4358-1
1.2479	2	0.2178+0	0.2265+1	0.8918+2	0.1574+1	0.3572+0
0.7907	3	0.4720-1	0.5909+0	0.2484+1	0.8794+2	0.1316+1
0.3632	4	0.7104-1	0.2081+0	0.1227+1	0.2866+1	0.8670+2

E = 2.5

E_{inc}	v_i \ v_f	0	1	2	3	4
2.5	0	0.9376+2	0.1491+1	0.1360+0	0.2165-1	0.1560-1
1.9843	1	0.1879+1	0.9020+2	0.1758+1	0.3086+0	0.6093-1
1.4979	2	0.2270+0	0.2329+1	0.8827+2	0.1708+1	0.4490+0
1.0407	3	0.5200-1	0.5885+0	0.2459+1	0.8651+2	0.1487+1
0.6132	4	0.6361-1	0.1971+0	0.1096+1	0.2524+1	0.8486+2

Table 3. The Elastic and Vibrational Transition Cross Sections of Electron-Hydrogen Molecule Scattering (Continued)

E = 2.75

E_{inc}	v_i \ v_f	0	1	2	3	4
2.75	0	0.9309+2	0.1553+1	0.1437+0	0.2563-1	0.1847-1
2.2343	1	0.1912+1	0.8888+2	0.1838+1	0.3311+0	0.7424-1
1.7479	2	0.2261+0	0.2350+1	0.8643+2	0.1799+1	0.5041+0
1.2907	3	0.5460-1	0.5732+0	0.2436+1	0.8427+2	0.1584+1
0.8632	4	0.5884-1	0.1921+0	0.1020+1	0.2368+1	0.8233+2

E = 3.0

E_{inc}	v_i \ v_f	0	1	2	3	4
3.0	0	0.9156+2	0.1576+1	0.1457+0	0.2823-1	0.2020-1
2.4843	1	0.1903+1	0.8692+2	0.1878+1	0.3401+0	0.8344-1
1.9979	2	0.2187+0	0.2336+1	0.8410+2	0.1854+1	0.5329+0
1.5407	3	0.5498+0	0.5484+0	0.2404+1	0.8162+2	0.1642+1
1.1132	4	0.5446-1	0.1862+0	0.9565+0	0.2273+1	0.7945+2

Table 3. The Elastic and Vibrational Transition Cross Sections of Electron-Hydrogen Molecule Scattering (Continued)

E = 3.25

E_{inc}	v_i \ v_f	0	1	2	3	4
3.25	0	0.8956+2	0.1571+1	0.1439+0	0.2963-1	0.2106-1
2.7343	1	0.1867+1	0.8467+2	0.1890+1	0.3400+0	0.8916-1
2.2479	2	0.2080+0	0.2299+1	0.8157+2	0.1881+1	0.5436+0
1.7907	3	0.5378-1	0.5191+0	0.2362+1	0.7884+2	0.1675+1
1.3632	4	0.5022-1	0.1788+0	0.8964+0	0.2201+1	0.7648+2

E = 3.5

E_{inc}	v_i \ v_f	0	1	2	3	4
3.5	0	0.8734+2	0.1550+1	0.1400+0	0.3012-1	0.2132-1
2.9843	1	0.1818+1	0.8231+2	0.1884+1	0.3343+0	0.9226-1
2.4979	2	0.1961+0	0.2251+1	0.7900+2	0.1891+1	0.5426+0
2.0407	3	0.5167-1	0.4889+0	0.2315+1	0.7607+2	0.1692+1
1.6132	4	0.4625	0.1706+0	0.8402+0	0.2140+1	0.7354+2

Table 3. The Elastic and Vibrational Transition Cross Sections of Electron-Hydrogen Molecule Scattering (Continued)

E = 3.75

E_{inc}	v_i \ v_f	0	1	2	3	4
3.75	0	0.8506+2	0.1521+1	0.1350+0	0.3002-1	0.2121-1
3.2343	1	0.1763+1	0.7995+2	0.1867+1	0.3257+0	0.9350-1
2.7479	2	0.1843+0	0.2198+1	0.7649+2	0.1889+1	0.5344+0
2.2907	3	0.4915-1	0.4599+0	0.2266+1	0.7338+2	0.1697+1
1.8632	4	0.4269-1	0.1623+0	0.7882+0	0.2087+1	0.7072+2

E = 4.0

E_{inc}	v_i \ v_f	0	1	2	3	4
4.0	0	0.8281+2	0.1487+1	0.1297+0	0.2953-1	0.2089-1
3.4843	1	0.1707+1	0.7766+2	0.1845+1	0.3156+0	0.9350-1
2.9979	2	0.1731+0	0.2144+1	0.7406+2	0.1879+1	0.5221+0
2.5407	3	0.4650-1	0.4328+0	0.2218+1	0.7082+2	0.1695+1
2.1132	4	0.3955-1	0.1541+0	0.7408+0	0.2038+1	0.6804+2

Table 3. The Elastic and Vibrational Transition Cross Sections of Electron-Hydrogen Molecule Scattering (Continued)

E = 4.25

E_{inc}	v_i \ v_f	0	1	2	3	4
4.25	0	0.8061+2	0.1453+1	0.1246+0	0.2884-1	0.2048-1
3.7343	1	0.1654+1	0.7545+2	0.1820+1	0.3051+0	0.9272-1
3.2479	2	0.1630+0	0.2093+1	0.7175+2	0.1866+1	0.5078+0
2.7907	3	0.4392-1	0.4083+0	0.2171+1	0.6839+2	0.1688+1
2.3632	4	0.3683-1	0.1465+0	0.6980+0	0.1993+1	0.6551+2

E = 4.5

E_{inc}	v_i \ v_f	0	1	2	3	4
4.5	0	0.7849+2	0.1421+1	0.1197+0	0.2805-1	0.2003-1
3.9843	1	0.1605+1	0.7333+2	0.1795+1	0.2950+0	0.9147-1
3.4979	2	0.1541+0	0.2044+1	0.6955+2	0.1849+1	0.4928+0
3.0407	3	0.4152-1	0.3865+0	0.2127+1	0.6609+2	0.1677+1
2.6132	4	0.3449-1	0.1394+0	0.6597+0	0.1952+1	0.6313+2

Table 3. The Elastic and Vibrational Transition Cross Sections of Electron-Hydrogen Molecule Scattering (Continued)

E = 4.75

E_{inc}	v_i \ v_f	0	1	2	3	4
4.75	0	0.7647+2	0.1390+1	0.1153+0	0.2724-1	0.1957-1
4.2343	1	0.1559+1	0.7130+2	0.1769+1	0.2854+0	0.8996-1
3.7479	2	0.1462+0	0.1999+1	0.6746+2	0.1830+1	0.4779+0
3.2907	3	0.3932-1	0.3672+0	0.2085+1	0.6393+2	0.1663+1
2.8632	4	0.3248-1	0.1330+0	0.6256+0	0.1912+1	0.6090+2

E = 5.0

E_{inc}	v_i \ v_f	0	1	2	3	4
5.0	0	0.7453+2	0.1361+1	0.1114+0	0.2644-1	0.1914-1
4.4843	1	0.1517+1	0.6937+2	0.1745+1	0.2765+0	0.8834-1
3.9979	2	0.1393+0	0.1957+1	0.6547+2	0.1811+1	0.4635+0
3.5407	3	0.3734-1	0.3502+0	0.2045+1	0.6188+2	0.1648+1
3.1132	4	0.3075-1	0.1272+0	0.5952+0	0.1874+1	0.5880+2

Table 3. The Elastic and Vibrational Transition Cross Sections of Electron-Hydrogen Molecule Scattering (Continued)

E = 5.25

E_{inc}	v_i \ v_f	0	1	2	3	4
5.25	0	0.7268+2	0.1334+1	0.1079+0	0.2568-1	0.1874-1
4.7343	1	0.1479+1	0.6753+2	0.1721+1	0.2685+0	0.8668-1
4.2479	2	0.1333+0	0.1918+1	0.6358+2	0.1791+1	0.4498+0
3.7907	3	0.3557-1	0.3353+0	0.2007+1	0.5995+2	0.1631+1
3.3632	4	0.2925-1	0.1220+0	0.5681+0	0.1838+1	0.5683+2

E = 5.5

E_{inc}	v_i \ v_f	0	1	2	3	4
5.5	0	0.7091+2	0.1309+1	0.1048+0	0.2498-1	0.1836-1
4.9843	1	0.1444+1	0.6577+2	0.1698+1	0.2612+0	0.8506-1
4.4979	2	0.1281+0	0.1881+1	0.6179+2	0.1770+1	0.4370+0
4.0407	3	0.3400-1	0.3222+0	0.1971+1	0.5812+2	0.1612+1
3.6132	4	0.2796-1	0.1173+0	0.5440+0	0.1803+1	0.5497+2

Table 3. The Elastic and Vibrational Transition Cross Sections of Electron-Hydrogen Molecule Scattering (Continued)

E = 5.75

E_{inc}	v_i \ v_f	0	1	2	3	4
5.75	0	0.6921+2	0.1286+1	0.1021+0	0.2433-1	0.1801-1
5.2343	1	0.1412+1	0.6409+2	0.1675+1	0.2545+0	0.8349-1
4.7479	2	0.1237+0	0.1847+1	0.6008+2	0.1749+1	0.4251+0
4.2907	3	0.3261-1	0.3105+0	0.1936+1	0.5639+2	0.1593+1
3.8632	4	0.2681-1	0.1131+0	0.5225+0	0.1769+1	0.5322+2

E = 6.0

E_{inc}	v_i \ v_f	0	1	2	3	4
6.0	0	0.6759+2	0.1264+1	0.9979-1	0.2374-1	0.1770-1
5.4843	1	0.1383+1	0.6248+2	0.1653+1	0.2486+0	0.8200-1
4.9979	2	0.1198+0	0.1814+1	0.5846+2	0.1727+1	0.4141+0
4.5407	3	0.3137-1	0.3002+0	0.1901+1	0.5474+2	0.1572+1
4.1132	4	0.2581-1	0.1093+0	0.5032+0	0.1735+1	0.5156+2

Table 3. The Elastic and Vibrational Transition Cross Sections of Electron-Hydrogen Molecule Scattering (Continued)

E = 6.5

E_{inc}	v_i \ v_f	0	1	2	3	4
6.5	0	0.6453+2	0.1223+1	0.9594-1	0.2271-1	0.1713-1
5.9843	1	0.1329+1	0.5946+2	0.1609+1	0.2382+0	0.7926-1
5.4979	2	0.1134+0	0.1752+1	0.5543+2	0.1682+1	0.3944+0
5.0407	3	0.2929-1	0.2829+0	0.1835+1	0.5170+2	0.1528+1
4.6132	4	0.2414-1	0.1028+0	0.4701+0	0.1669+1	0.4852+2

E = 7.0

E_{inc}	v_i \ v_f	0	1	2	3	4
7.0	0	0.6171+2	0.1186+1	0.9297-1	0.2186-1	0.1666-1
6.4843	1	0.1280+1	0.5668+2	0.1566+1	0.2297+0	0.7682-1
5.9979	2	0.1085+0	0.1693+1	0.5266+2	0.1635+1	0.3774+0
5.5407	3	0.2762-1	0.2688+0	0.1770+1	0.4896+2	0.1481+1
5.1132	4	0.2280-1	0.9742-1	0.4427+0	0.1604+1	0.4579+2

Table 3. The Elastic and Vibrational Transition Cross Sections of Electron-Hydrogen Molecule Scattering (Continued)

E = 7.5

E_{inc}	v_i \ v_f	0	1	2	3	4
7.5	0	0.5909+2	0.1150+1	0.9056-1	0.2114-1	0.1623-1
6.9843	1	0.1235+1	0.5413+2	0.1522+1	0.2222+0	0.7463-1
6.4979	2	0.1045+0	0.1636+1	0.5013+2	0.1586+1	0.3623+0
6.0407	3	0.2625-1	0.2570+0	0.1706+1	0.4646+2	0.1432+1
5.6132	4	0.2169-1	0.9286-1	0.4194+0	0.1541+1	0.4332+2

E = 8.0

E_{inc}	v_i \ v_f	0	1	2	3	4
8.0	0	0.5667+2	0.1115+1	0.8850-1	0.2052-1	0.1584-1
7.4843	1	0.1192+1	0.5177+2	0.1478+1	0.2157+0	0.7265-1
6.9979	2	0.1011+0	0.1581+1	0.4781+2	0.1537+1	0.3487+0
6.5407	3	0.2510-1	0.2469+0	0.1645+1	0.4418+2	0.1383+1
6.1132	4	0.2073-1	0.8894-1	0.3992+0	0.1480+1	0.4108+2

Table 3. The Elastic and Vibrational Transition Cross Sections of Electron-Hydrogen Molecule Scattering (Continued)

E = 8.5

E_{inc}	v_i \ v_f	0	1	2	3	4
8.5	0	0.5441+2	0.1083+1	0.8667-1	0.2008-1	0.1550-1
7.9843	1	0.1153+1	0.4958+2	0.1434+1	0.2107+0	0.7090-1
7.4979	2	0.9825-1	0.1527+1	0.4568+2	0.1483+1	0.3377+0
7.0407	3	0.2424-1	0.2390+0	0.1580+1	0.4211+2	0.1328+1
6.6132	4	0.1992-1	0.8561-1	0.3829+0	0.1414+1	0.3907+2

E = 9.0

E_{inc}	v_i \ v_f	0	1	2	3	4
9.0	0	0.5230+2	0.1052+1	0.8502-1	0.1970-1	0.1517-1
8.4843	1	0.1116+1	0.4754+2	0.1390+1	0.2064+0	0.6930-1
7.9979	2	0.9567-1	0.1475+1	0.4372+2	0.1429+1	0.3280+0
7.5407	3	0.2351-1	0.2322+0	0.1515+1	0.4023+2	0.1271+1
7.1132	4	0.1920-1	0.8265-1	0.3688+0	0.1348+1	0.3725+2

Table 3. The Elastic and Vibrational Transition Cross Sections of Electron-Hydrogen Molecule Scattering (Continued)

E = 9.5

E_{inc}	v_i \ v_f	0	1	2	3	4
9.5	0	0.5033+2	0.1022+1	0.8352-1	0.1934-1	0.1486-1
8.9843	1	0.1081+1	0.4565+2	0.1347+1	0.2021+0	0.6777-1
8.4979	2	0.9337-1	0.1424+1	0.4190+2	0.1375+1	0.3187+0
8.0407	3	0.2286-1	0.2259+0	0.1454+1	0.3849+2	0.1217+1
7.6132	4	0.1855-1	0.7997-1	0.3557+0	0.1286+1	0.3559+2

E = 10.0

E_{inc}	v_i \ v_f	0	1	2	3	4
10.0	0	0.4849+2	0.9926+0	0.8208-1	0.1900-1	0.1456-1
9.4843	1	0.1046+1	0.4390+2	0.1304+1	0.1980+0	0.6629-1
8.9979	2	0.9123-1	0.1374+1	0.4022+2	0.1324+1	0.3098+0
8.5407	3	0.2225-1	0.2198+0	0.1395+1	0.3689+2	0.1165+1
8.1132	4	0.1795-1	0.7749-1	0.3436+0	0.1227+1	0.3405+2

In TABLE 4, the e-D_2 vibrational elastic and inelastic cross sections are tabulated. The units and the notations are the same as in TABLE 3 except that the ε_{v_i} is the vibrational energy level of D_2. These cross section data were generated using the same interaction potential as described in SECTION II. The vibrational wave functions $\phi_v(R)$ of D_2 were computed again from Hulbert-Hirschfelder energy curve (Ref.15).

The vibrational excitation cross sections $\sigma_{0\to v}$ of e-H_2 for v=1,2,3 are shown in Figure 4. No substructures appear in these cross sections in contrast to the e-N_2, CO cases. The cross sections show broad resonances between 2∿4 eV. The 0→1 transition is dominant and the excitation cross sections, in general, decreases faster than corresponding e-N_2, CO cross sections as $\Delta v=v_f-v_i$ increases. In Figure 5, the vibrational excitation cross sections from the initially first excited state $\sigma_{1\to v}$ with v=2,3,4 are shown. Again, 1→2 excitation cross section is the largest one among these cross sections and the trend of the contribution in terms of Δv is similar to the 0→v case. However, the broad resonance peaks are shifted to somewhat lower energy region. In Figure 6, where the excitation cross sections from initially second excited state $\sigma_{2\to v}$ with v=3,4 are shown, these features are the same as above and the broad resonance peaks are shifted toward lower energy region again. For the present e-N_2,D_2 vibrational excitation cross sections decrease so fast, as Δv increases, that the cross sections for $\Delta v > 3$ are practically negligible.

TABLE 4

THE ELASTIC AND VIBRATIONAL TRANSITION CROSS SECTIONS OF ELECTRON-DEUTERON MOLECULE SCATTERING

E = 1.0

E_{inc}	v_i \ v_f	0	1	2
1.0	0	0.5964+2	0.6185+0	0.1470-1
0.6290	1	0.9832+0	0.6257+2	0.8551+0
0.2730	2	0.5385-1	0.1970+1	0.6538+2

E = 1.5

E_{inc}	v_i \ v_f	0	1	2	3	4
1.5	0	0.7767+2	0.7461+0	0.2889-1	0.2455-2	0.6925-3
1.1290	1	0.9913+0	0.7862+2	0.1080+1	0.8663-1	0.4356-2
0.7730	2	0.5607-1	0.1578+1	0.8024+2	0.1215+1	0.9634-1
0.4316	3	0.8533-2	0.2266+0	0.2177+1	0.8132+2	0.8998+0
0.1048	4	0.9914-2	0.4693-1	0.7108+0	0.3706+1	0.8166+2

E = 2.0

E_{inc}	v_i \ v_f	0	1	2	3	4
2.0	0	0.9075+2	0.1034+1	0.5449-1	0.5192-2	0.2540-2
1.6290	1	0.1269+1	0.8953+2	0.1432+1	0.1675+0	0.1573-1
1.2730	2	0.8561-1	0.1832+1	0.8958+2	0.1615+1	0.2624+0
0.9316	3	0.1114-1	0.2930+0	0.2207+1	0.8924+2	0.1516+1
0.6048	4	0.8402-2	0.4237-1	0.5524+0	0.2335+1	0.8811+2

Table 4. The Elastic and Vibrational Transition Cross Sections of Electron-Deuteron Scattering (Continued)

E = 2.5

E_{inc}	v_i \ v_f	0	1	2	3	4
2.5	0	0.9459+2	0.1257+1	0.7378-1	0.9622-2	0.4486-2
2.1290	1	0.1476+1	0.9170+2	0.1719+1	0.2219+0	0.2957-1
1.7730	2	0.1040+0	0.2064+1	0.9036+2	0.1939+1	0.3616+0
1.4316	3	0.1680-1	0.3300+0	0.2401+1	0.8895+2	0.1814+1
1.1048	4	0.1015-1	0.5698-1	0.5804+0	0.2350+1	0.8702+2

E = 3.0

E_{inc}	v_i \ v_f	0	1	2	3	4
3.0	0	0.9252+2	0.1317+1	0.7726-1	0.1230-1	0.5401-2
2.6290	1	0.1503+1	0.8885+2	0.1809+1	0.2308+0	0.3712-1
2.2730	2	0.1019+0	0.2093+1	0.8671+2	0.2055+1	0.3861+0
1.9316	3	0.1910-1	0.3141+0	0.2419+1	0.8468+2	0.1944+1
1.6048	4	0.1009-1	0.6081-1	0.5470+0	0.2340+1	0.8236+2

Table 4. The Elastic and Vibrational Transition Cross Sections of Electron-Deuteron Molecule Scattering (Continued)

E = 3.5

E_{inc}	v_i \ v_f	0	1	2	3	4
3.5	0	0.8831+2	0.1283+1	0.7280-1	0.1272-1	0.5389-2
3.1290	1	0.1435+1	0.8443+2	0.1786+1	0.2179+0	0.3851-1
2.7730	2	0.9188-1	0.2016+1	0.8190+2	0.2048+1	0.3713+0
2.4316	3	0.1831-1	0.2804+0	0.2336+1	0.7952+2	0.1966+1
2.1048	4	0.8962-2	0.5725-1	0.4892+0	0.2271+1	0.7696+2

E = 4.0

E_{inc}	v_i \ v_f	0	1	2	3	4
4.0	0	0.8376+2	0.1221+1	0.6650-1	0.1205-1	0.5018-2
3.6290	1	0.1346+1	0.7986+2	0.1727+1	0.2000+0	0.3705-1
3.2730	2	0.8127-1	0.1914+1	0.7714+2	0.1998+1	0.3450+0
2.9316	3	0.1645-1	0.2476+0	0.2230+1	0.7455+2	0.1942+1
2.6048	4	0.7706-2	0.5161-1	0.4335+0	0.2186+1	0.7182+2

Table 4. The Elastic and Vibrational Transition Cross Sections of Electron-Deuteron Molecule Scattering (Continued)

E = 4.5

E_{inc}	v_i \ v_f	0	1	2	3	4
4.5	0	0.7943+2	0.1158+1	0.6078-1	0.1108-1	0.4598-2
4.1290	1	0.1262+1	0.7557+2	0.1663+1	0.1837+0	0.3474-1
3.7730	2	0.7249-1	0.1820+1	0.7274+2	0.1938+1	0.3188+0
3.4316	3	0.1453-1	0.2210+0	0.2131+1	0.7001+2	0.1903+1
3.1048	4	0.6664-2	0.4621-1	0.3875+0	0.2103+1	0.6716+2

E = 5.0

E_{inc}	v_i \ v_f	0	1	2	3	4
5.0	0	0.7545+2	0.1103+1	0.5623-1	0.1015-1	0.4227-2
4.6290	1	0.1192+1	0.7164+2	0.1605+1	0.1705+0	0.3246-1
4.2730	2	0.6579-1	0.1738+1	0.6874+2	0.1881+1	0.2965+0
3.9316	3	0.1290-1	0.2008+0	0.2044+1	0.6592+2	0.1859+1
3.6048	4	0.5863-2	0.4168-1	0.3515+0	0.2028+1	0.6299+2

Table 4. The Elastic and Vibrational Transition Cross Sections of Electron-Deuteron Molecule Scattering (Continued)

E = 5.5

E_{inc}	v_i \ v_f	0	1	2	3	4
5.5	0	0.7182+2	0.1057+1	0.5279-1	0.9356-2	0.3926-2
5.1290	1	0.1134+1	0.6804+2	0.1554+1	0.1604+0	0.3049-1
4.7730	2	0.6083-1	0.1669+1	0.6510+2	0.1828+1	0.2784+0
4.4316	3	0.1161-1	0.1856+0	0.1969+1	0.6223+2	0.1815+1
4.1048	4	0.5260-2	0.3810-1	0.3238+0	0.1960+1	0.5925+2

E = 6.0

E_{inc}	v_i \ v_f	0	1	2	3	4
6.0	0	0.6849+2	0.1017+1	0.5031-1	0.8701-2	0.3690-2
5.6290	1	0.1084+1	0.6474+2	0.1508+1	0.1525+0	0.2888-1
5.2730	2	0.5725-1	0.1610+1	0.6179+2	0.1778+1	0.2640+0
4.9316	3	0.1058-1	0.1741+0	0.1901+1	0.5888+2	0.1770+1
4.6048	4	0.4809-2	0.3530-1	0.3023+0	0.1895+1	0.5588+2

Table 4. The Elastic and Vibrational Transition Cross Sections of Electron-Deuteron Molecule Scattering (Continued)

E = 7.0

E_{inc}	v_i \ v_f	0	1	2	3	4
7.0	0	0.6259+2	0.9515+0	0.4725-1	0.7759-2	0.3373-2
6.6290	1	0.1004+1	0.5891+2	0.1424+1	0.1416+0	0.2654-1
6.2730	2	0.5273-1	0.1505+1	0.5597+2	0.1681+1	0.2429+0
5.9316	3	0.9157-2	0.1583+0	0.1778+1	0.5307+2	0.1675+1
5.6048	4	0.4213-2	0.3139-1	0.2718+0	0.1772+1	0.5009+2

E = 8.0

E_{inc}	v_i \ v_f	0	1	2	3	4
8.0	0	0.5753+2	0.8936+0	0.4547-1	0.7136-2	0.3159-2
7.6290	1	0.9370+0	0.5394+2	0.1344+1	0.1342+0	0.2497-1
7.2730	2	0.5001-1	0.1410+1	0.5105+2	0.1585+1	0.2296+0
6.9316	3	0.8236-2	0.1477+0	0.1663+1	0.4819+2	0.1575+1
6.6048	4	0.3827-2	0.2885-1	0.2507+0	0.1653+1	0.4529+2

Table 4. The Elastic and Vibrational Transition Cross Sections of Electron-Deuteron Molecule Scattering (Continued)

E = 9.0

E_{inc}	v_i \ v_f	0	1	2	3	4
9.0	0	0.5313+2	0.8428+0	0.4393-1	0.6794-2	0.2945-2
8.6290	1	0.8791+0	0.4964+2	0.1270+1	0.1292+0	0.2397-1
8.2730	2	0.4779-1	0.1325+1	0.4683+2	0.1487+1	0.2173+0
7.9316	3	0.7709-2	0.1406+0	0.1551+1	0.4408+2	0.1466+1
7.6048	4	0.3485-2	0.2720-1	0.2365+0	0.1529+1	0.4129+2

E = 10.0

E_{inc}	v_i \ v_f	0	1	2	3	4
10.0	0	0.4929+2	0.7948+0	0.4268-1	0.6527-2	0.2779-2
9.6290	1	0.8254+0	0.4591+2	0.1197+1	0.1247+0	0.2314-1
9.2730	2	0.4603-1	0.1243+1	0.4320+2	0.1391+1	0.2083+0
8.9316	3	0.7307-2	0.1344+0	0.1444+1	0.4056+2	0.1361+1
8.6048	4	0.3230-2	0.2589-1	0.2244+0	0.1412+1	0.3790+2

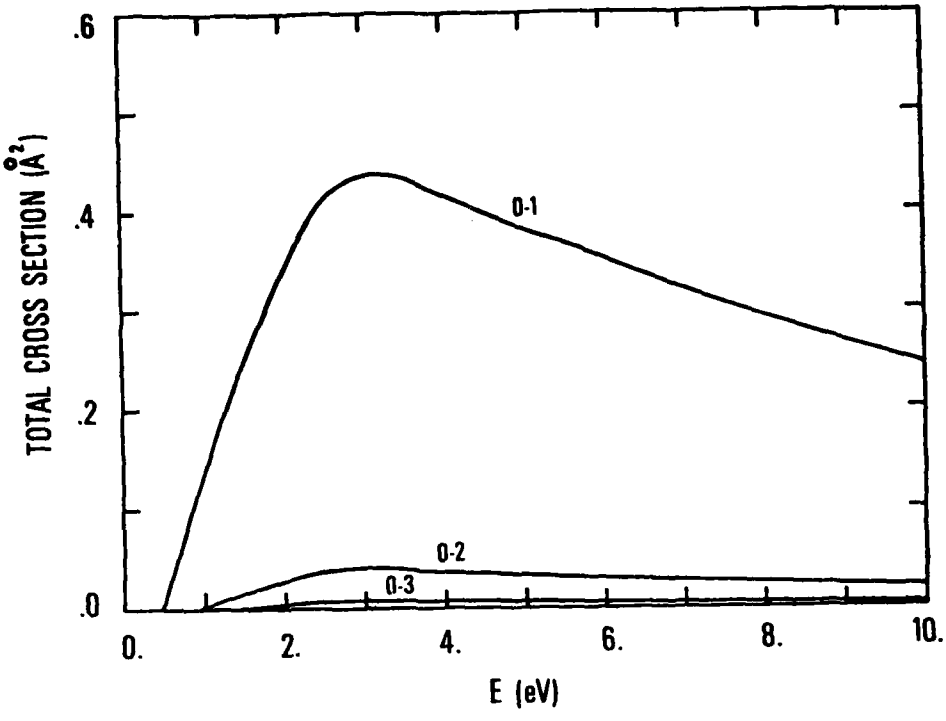

Figure 4. The Vibrational Excitation Cross Sections $\sigma_{0\to v}$ for v = 1,2,3.

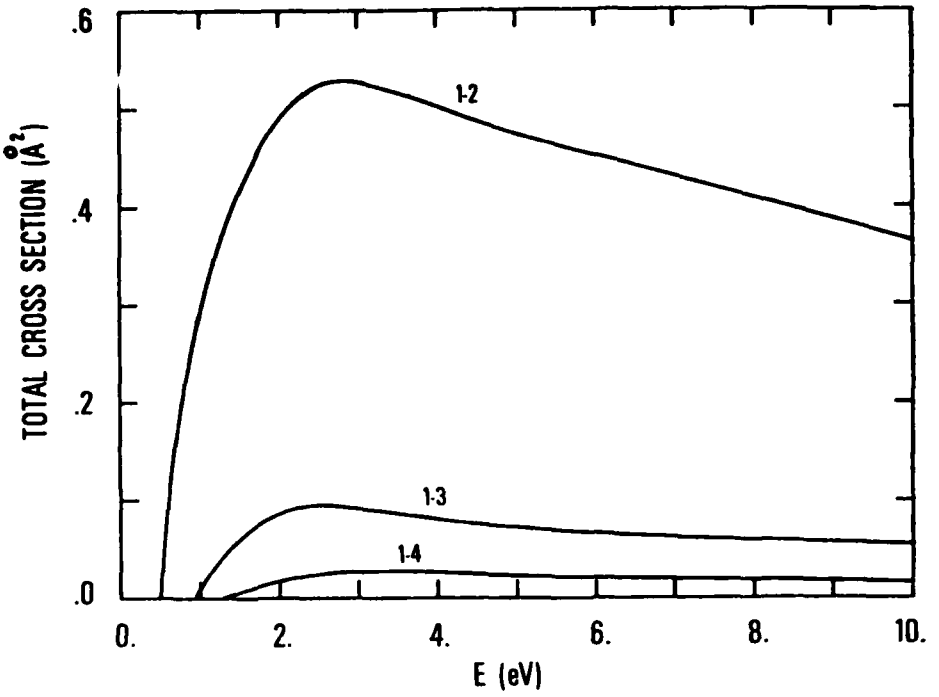

Figure 5. The Vibrational Excitation Cross Sections $\sigma_{1\to v}$ for v = 2,3,4.

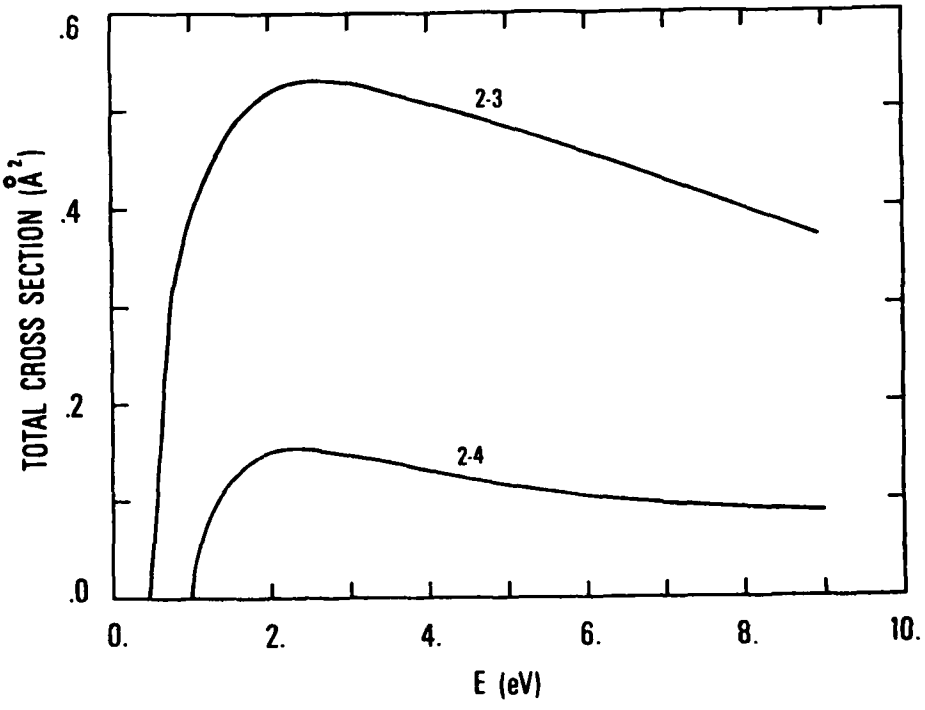

Figure 6. The Vibrational Excitation Cross Sections $\sigma_{2\to v}$ for v = 3,4.

The differential cross sections for the vibrational elastic scattering and excitation obtained from present calculation are shown in Figures 7∿11 . The shapes of the differential cross sections from the present theory are basically similar to each other in the resonance region. They have minima around 90^{o} and both forward and backward peaks. This indicates that the $e\text{-}N_2, D_2$ resonances are of $p\sigma_u$-wave character. The theoretical shapes of the differential cross sections of the vibrationally elastic and inelastic scattering are consistent with the experimental measurements on the differential cross sections of the rotational excitation (Ref. 16).

The rate coefficients $k_{v_i \to v_f}$ of the elastic scattering and vibrational excitation evaluated from the present cross sections for kT = 0.5, 1.0, 1.5 and 2.0 eV are tabulated in TABLE 5 and TABLE 6 for $e\text{-}H_2$ and D_2, respectively. The entries of these tables are in units of cm^3/sec. The numbers a-n should read as $ax10^{-n}$. For the integration over the energies to get the rate coefficients, we made linear interpolation between calculated cross sections. Thus, the entries in these tables are approximate values. Yet, the general trend of the vibrational excitations can be found from these tables. The rate coefficients of the vibrational deexcitation may be obtained from

$$k_{v_f \to v_i} = k_{v_i \to v_f} \times e^{\frac{\varepsilon_{v_f} - \varepsilon_{v_i}}{kT}} \qquad (27)$$

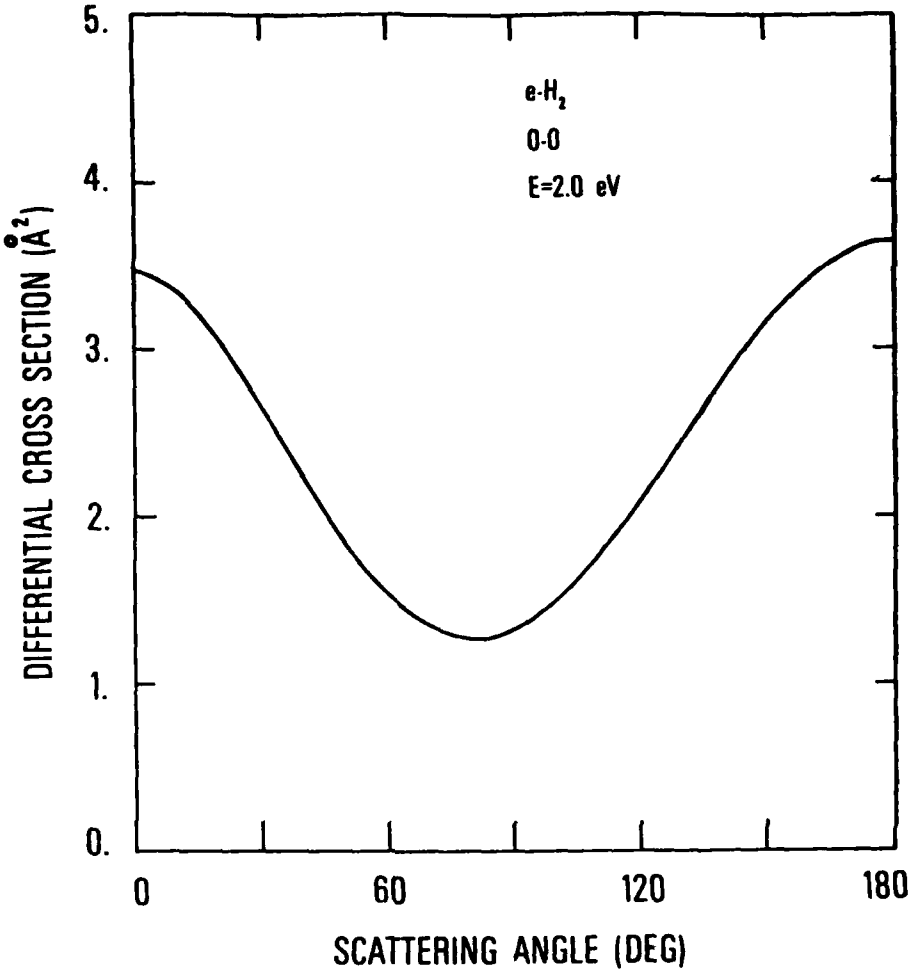

Figure 7. Differential Cross Section for Elastic Scattering at E = 2.0 eV.

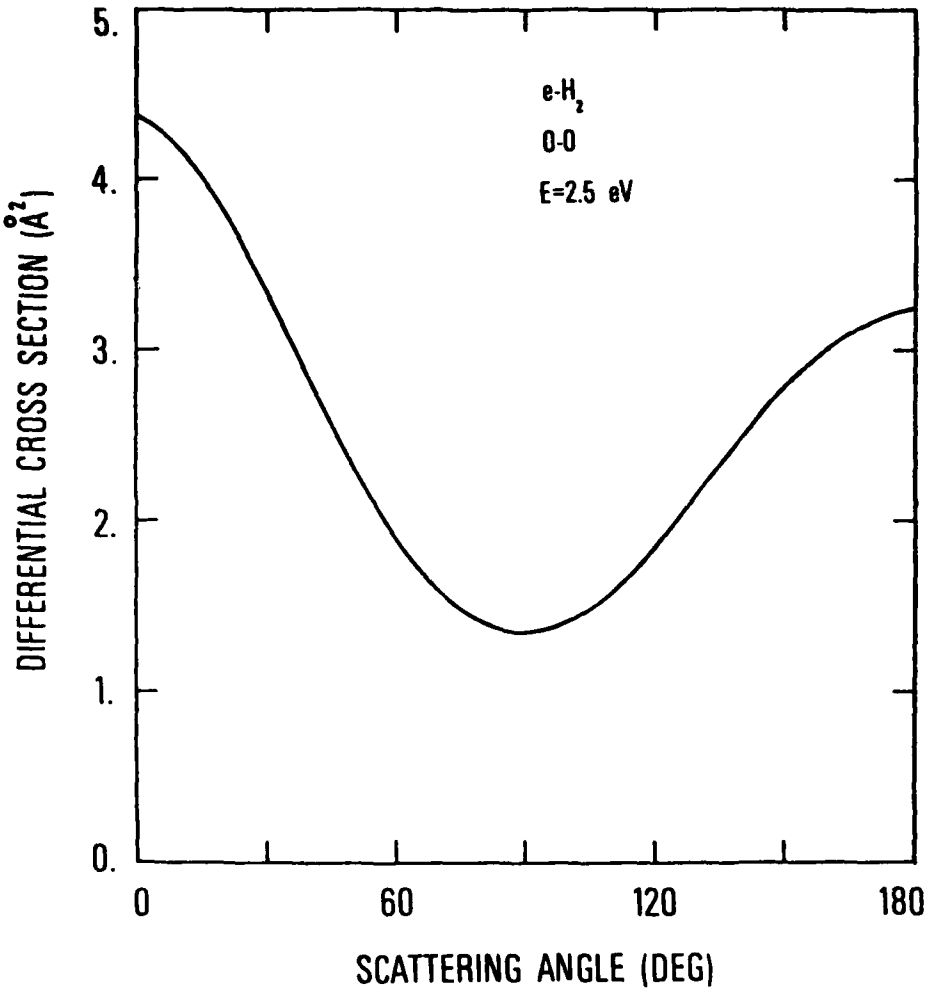

Figure 8. Differential Cross Section for Elastic Scattering at E = 2.5 eV.

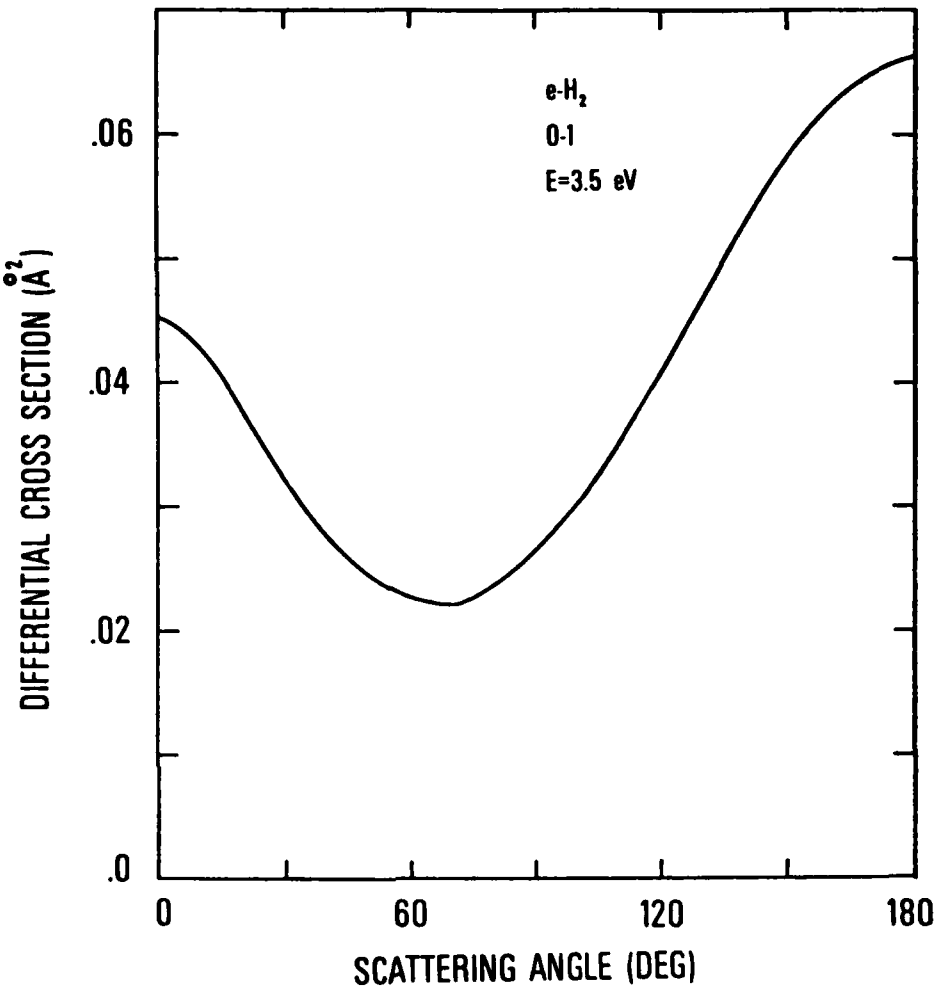

Figure 9. Differential Cross Section for 0→1 Vibrational Excitation at E = 3.5 eV.

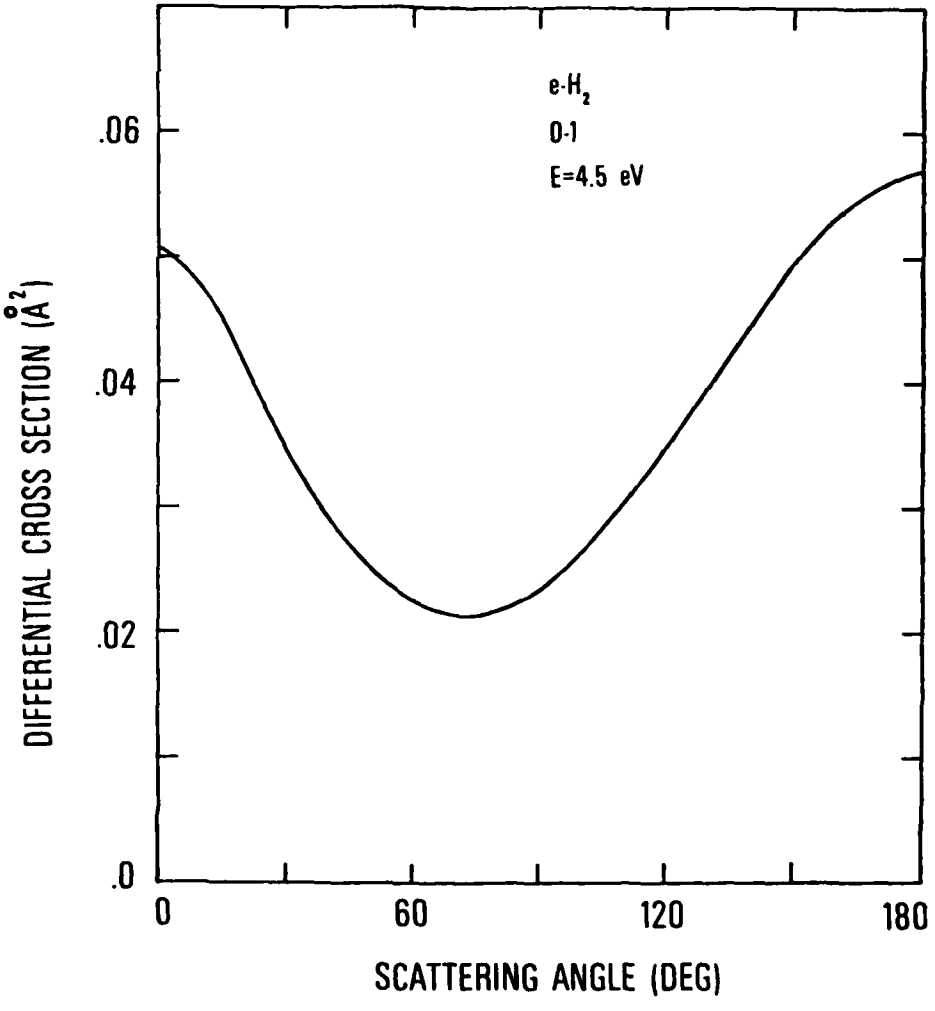

Figure 10. Differential Cross Section for 0→1 Vibrational Excitation at E = 4.5 eV.

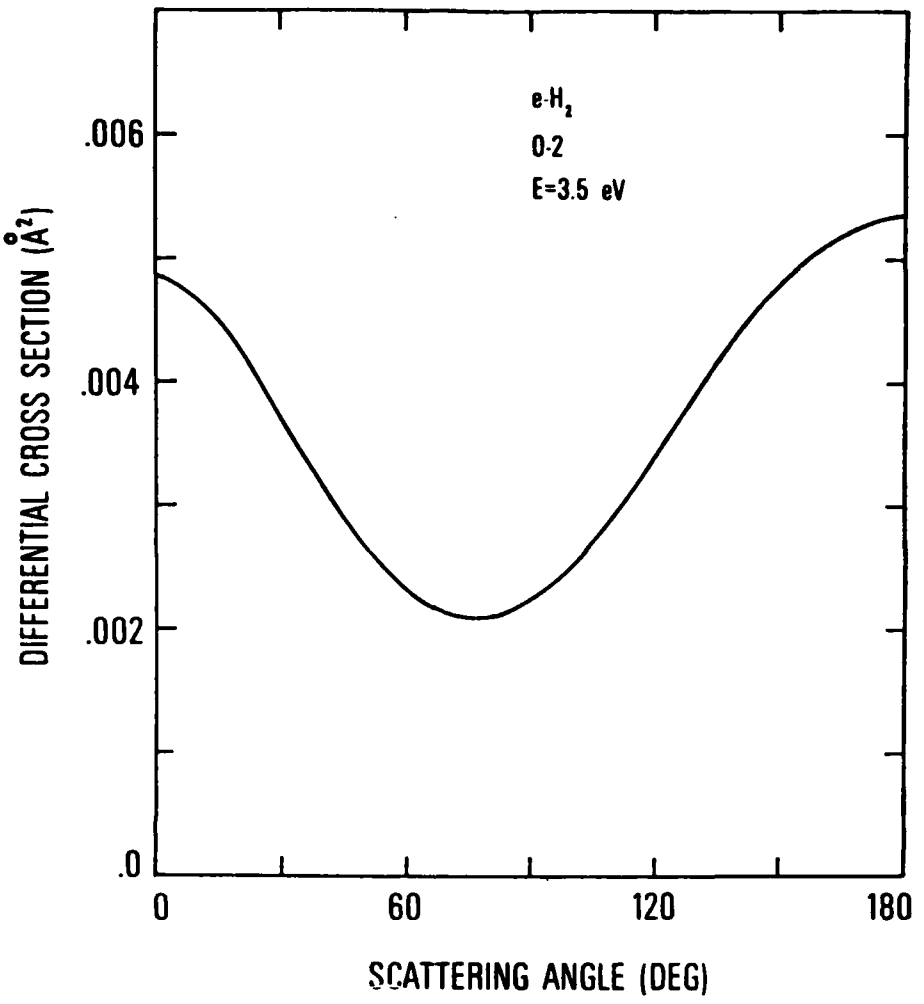

Figure 11. Differential Cross Section for 0→2 Vibrational Excitation at E = 3.5 eV.

TABLE 5

THE RATE COEFFICIENTS OF ELASTIC SCATTERING AND VIBRATIONAL TRANSITIONS FOR ELECTRON-HYDROGEN MOLECULE

v_i \ v_f	0	1	2	3	4
	kT=0.5				
0	0.7042-7	0.7363-9	0.3239-10	0.3394-11	0.1791-11
1		0.9710-7	0.1122-8	0.1150-9	0.1621-10
2			0.1081-6	0.1369-8	0.2332-9
				0.1097-6	0.1401-8
					0.1047-6
	kT=1.0				
0	0.1357-6	0.1825-8	0.1272-9	0.2013-10	0.1305-10
1		0.1477-6	0.2527-8	0.3617-9	0.7728-10
2			0.1491-6	0.2780-8	0.6415-9
3				0.1425-6	0.2644-8
4					0.1318-6
	kT=1.5				
0	0.1731-6	0.2596-8	0.1995-9	0.3621-10	0.2472-10
1		0.1741-6	0.3435-8	0.5244-9	0.1295-9
2			0.1682-6	0.3638-8	0.8863-9
3				0.1564-6	0.3353-8
4					0.1426-6
	kT=2.0				
0	0.1928-6	0.3064-8	0.2429-9	0.4711-10	0.3295-10
1		0.1861-6	0.3958-8	0.6139-9	0.1629-9
2			0.1750-6	0.4100-8	0.1010-8
3				0.1600-6	0.3703-8
4					0.1443-6

TABLE 6

THE RATE COEFFICIENTS OF ELASTIC SCATTERING AND VIBRATIONAL TRANSITIONS FOR ELECTRON-DEUTERON MOLECULE

v_i \ v_f	0	1	2	3	4
	kT=0.5				
0	0.6354-7	0.5985-9	0.2089-10	0.1805-11	0.7104-12
1		0.8570-7	0.1139-8	0.8480-10	0.8166-11
2			0.1016-6	0.1416-8	0.1862-9
3				0.1058-6	0.1616-8
4					0.1062-6
	kT=1.0				
0	0.1340-6	0.1524-8	0.7125-10	0.9055-11	0.3843-11
1		0.1444-6	0.2415-8	0.2486-9	0.3342-10
2			0.1498-6	0.2938-8	0.4657-9
3				0.1486-6	0.3022-8
4					0.1427-6
	kT=1.5				
0	0.1736-6	0.2158-8	0.1078-9	0.1540-10	0.6580-11
1		0.1753-6	0.3251-8	0.3516-9	0.5315-10
2			0.1739-6	0.3865-8	0.6260-9
3				0.1680-6	0.3860-8
4					0.1585-6
	kT=2.0				
0	0.1943-6	0.2534-8	0.1292-9	0.1941-10	0.8302-11
1		0.1900-6	0.3732-8	0.4064-9	0.6502-10
2			0.1841-6	0.4372-8	0.7054-9
3				0.1749-6	0.4299-8
4					0.1630-6

As Δv increases, the $k_{v_i \to v_f}$ decreases fast as expected from the behavior of the cross sections. The rate coefficients of e-H_2 and D_2 are in the same order of magnitude. No special isotope effects can be found in these rate coefficients.

Comparison between available experimental measurements and the results of the present calculation on the 0 1 vibrational excitation cross section of e-H_2 scattering are made in Figure 12. The experimental data were taken from the works of Linder and Schmidt (Ref. 17), and Ehrhardt, Langhans, Linder and Taylor (Ref. 18). There exist some discrepancies between the experimental results. The present theoretical cross sections are seen in good agreement with the experimental data in the resonance region. At higher energies around 10 eV, the experimental data is somewhat lower than our theortical results.

In Figure 13, our results are compared with the experimental data on the 0→2 vibrational excitation cross sections. The experimental data were taken from Ref. 18 above 1.5 eV of the energy and from the work of Burrow and Schulz (Ref. 19) between threshold and 1.5 eV of the energy. Our results are in good agreement with the experimental ones. The 0→3 vibrational excitation cross sections of the present calculations are compared with the experimental data in Figure 14. The experimental data were taken from Ref. 18 above 2 eV of energy and from Ref. 19 near threshold. Whereas the energy dependences of the cross sections were close to each other, the absolute magnitudes of the present results and the

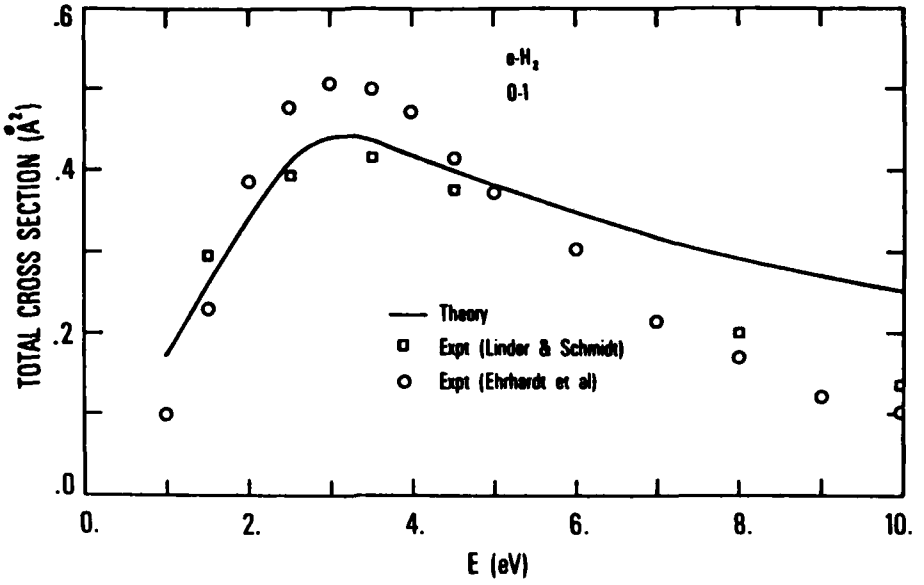

Figure 12. Comparison Between the Experiments and Theory for 0→1 Vibrational Excitation Cross Section.

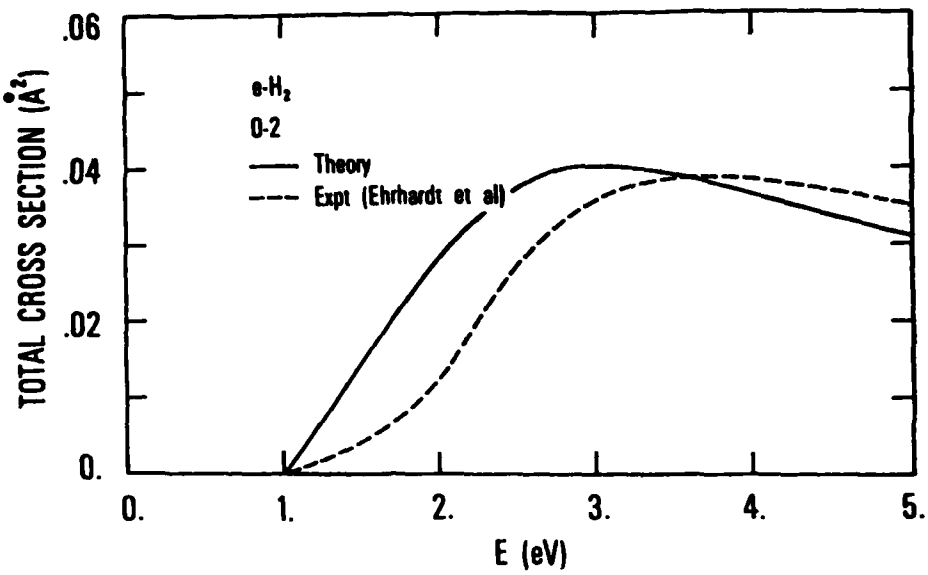

Figure 13. Comparison Between the Experiment and Theory for 0→2 Vibrational Excitation Cross Section.

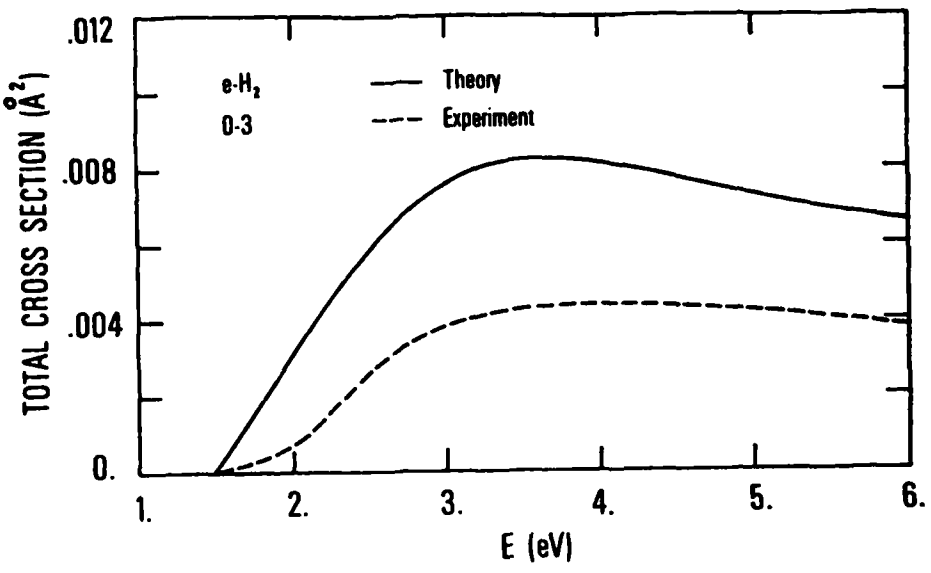

Figure 14. Comparison Between the Experiment and Theory for 0→3 Vibrational Excitation Cross Section.

experimental ones roughly differ by a factor of 2. In Figure 15, the present vibrationally elastic cross sections are compared with the experimental measurements by Linder and Schmidt (Ref. 18). The energy dependences of the cross sections are quite close to each other, but again the present theory of the available experiment gives results differing by approximately a factor of 2.

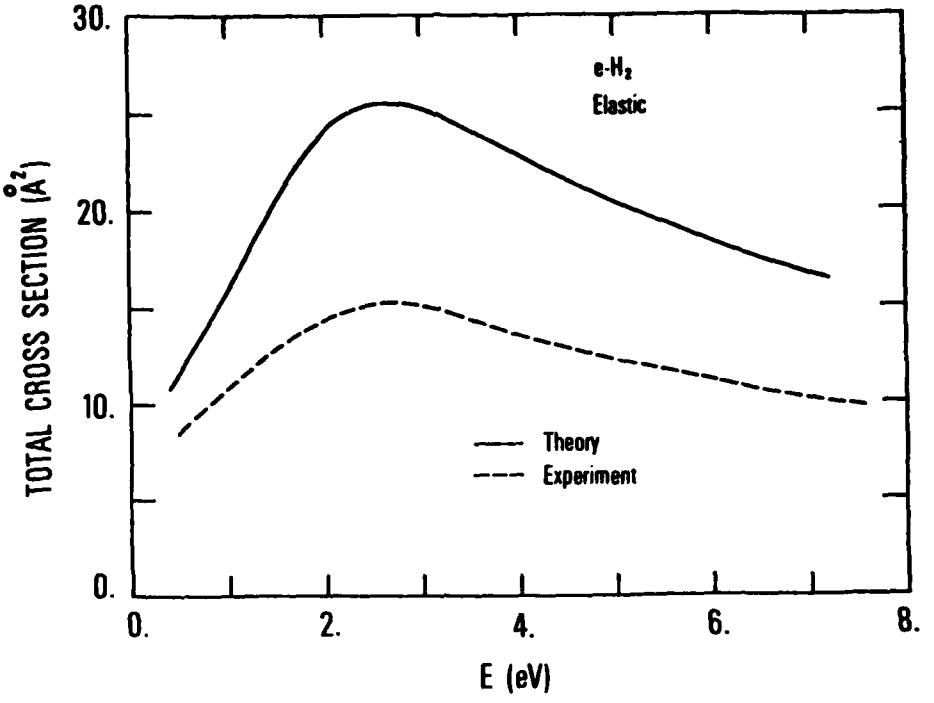

Figure 15. Comparison Between the Experiment and Theory for Vibrationally Elastic Scattering Cross Sections.

SECTION IV

DISCUSSION AND CONCLUSION

In this work, we have carried out calculations on the vibrational transition cross sections of e-H_2,D_2 scatterings in the energy range of 0 $\sim$ 10 eV employing the simultaneous vibrational and rotational adiabatic approach. Also, we have applied the hybrid theory for the present systems, and the results on the elastic and vibrational transition cross sections re found to be not satisfactory. The cross sections obtained from the hybrid theory show sharp peaks below the resonance region, which are in contrast to the results of the experimental measurements where the resonance peaks are quite broad between 2 $\sim$ 3 eV for the vibrationally elastic scattering and around 3 eV for the vibrational excitations.

In electron-heavy target molecule scattering such as e-CO or N_2, the vibrational motion of target is much faster than the rotational motion. The hybrid theory where the vibrational degree of freedom is treated with dynamic coupling and the rotational one is taken into account by adiabatic approximation yields results in good agreement with experiment, especially in predicting the peak structures of cross sections.

For electron-light target molecule scatterings such as e-H_2,D_2, the vibrational and rotational motions are comparable to each other, namely, the rotational motion is as fast as the vibrational one. This can be seen from the numbers of the

rotational energy levels within the vibrational energy range $\Delta\varepsilon_v = \varepsilon_{v+1} - \varepsilon_v$ for the above molecules.

Experimentally, no oscillating structure is observed in e-H_2 case as is characterized in e-N_2 and e-CO cases. The physical interpretation of the experimental results could be that the substructures of the cross sections due to fast vibrational motion of target molecule are smeared out because of the rotational motion.

Therefore, the vibrational and rotational motions must be treated with the same degrees of approximation in the scattering of light target molecules. For this reason, the simultaneous vibrational and rotational adiabatic approach, which we adopted here, is more appropriate. In addition, it is computationally much less complicated than the Hybrid Theory approach.

Among the vibrational transition cross sections, the one with $\Delta v = 1$ is dominant and the cross sections decrease monotonically as Δv increases. The present e-H_2,D_2 vibrational transition cross sections decrease much faster than those of e-CO, N_2 case as Δv increases and thus the cross sections with $v \geq 5$ are practically negligible. In the theoretical cross sections reported here, the ones with $\Delta v = 4$ (0→4 transition) is expected to be less accurate than the other cross sections. The reason is that the molecular orbital wave functions published so far are available only for a limited range of the internuclear separation R, which is not sufficient to cover the entire vibrational stretching of $v = 4$ state. We made appropriate extrapolation from the available wave functions.

The energy dependences of the present e-H_2 cross sections are quite smooth in the 0-10 eV region and the resonances are of broad natures. The e-D_2 cross sections are qualitatively similar to the e-H_2 case. It seems that there exists no particular isotopic effects between these two electron-molecule systems.

One could obtain the vibrational transition cross sections including higher vibrational states with $v \geq 5$ employing those extrapolated molecular wave functions. However, the energy separations of the vibrational states in H_2, D_2 molecules are quite wide and thus the higher vibrational states of the ground electronic state $X^1\Sigma_g$ of H_2, D_2 molecules begin to overlap with the dissociative wave function of the (repulsive) excited electronic state $b^3\Sigma_u$ of H_2, D_2. We have to include those wave functions as well in order to obtain reliable transition cross sections of the higher vibrational states, and this is not a simple task. Therefore, in this report, we have not considered the transition cross sections with the inclusion of the higher vibrational states for $v \geq 5$.

In this work we have made some exploration on the e-O_2 vibrational transition cross sections. A qualitative discussion is given in the following.

We have explored the e-O_2 vibrational transition cross sections for the incident energies between E ≃ 0-1eV, which corresponds to the higher vibrational states (v' ≥ 3). Here, the vibrational excitation cross sections are dominated by the existence of the compound electronic state $X^2\Pi_g$ of O_2^-. The direct excitation mechanism contributes a small amount to the cross sections. Thus, when the vibrational close-coupling theory is applied to compute the cross sections, large numbers of closed channels should be included and the convergence of the basis states is expected to be very slow. The theoretical study of the e-O_2 vibrational transitions becomes quite a complex problem. Therefore, we analyze them only qualitatively based on the available experimental measurements.

When the target molecule O_2 is in its ground vibrational state, the resonance peaks appear at around E ≃ 0.32, 0.44, 0.56, 0.68, 0.79, 0.90, 1.02, 1.13, 1.24 eV of the incident energies in the 0→1 vibrational excitation cross sections, which correspond to the vibrational states v' = 6∿14 of the compound molecule. For the 0→2 excitation, the resonance peaks occur at E = 0.56, 0.68, 0.79, 0.92, 1.02, 1.13, 1.24, 1.34, 1.45 eV corresponding to v' = 8∿16 of the compound vibrational states. For the 0→3 transition, those peaks appear at E = 0.79, 0.92, 1.02, 1.13, 1.24, 1.34, 1.45, 1.54, 1.64 eV. These peaks are again associated with the vibrational states v' = 10∿18 of the compound molecule. The cross section will decrease monotonically as v increase. The above resonance peaks and the relative

magnitudes of the cross sections are confirmed by the experiment (Ref. 20) and strongly sgugest that the vibrational transitions occur mainly via the compound molecule. Thus, one can predict some behaviors of the cross sections. For example, when the target molecule O_2 is in the first excited vibrational state (v=1), for which no experimental data are available, the rsonance peaks will appear at E = 0.12, 0.24, 0.36, 0.48, 0.59, 0.70, 0.82, 0.93, 1.04 eV in the 1→2 vibrational excitation cross sections and these correspond to v' = 6∿14 of the compound molecule. For the 1→3 excitation, those peaks will appear at E = 0.36, 0.48, 0.59, 0.72, 0.82, 0.93, 1.04, 1.14, 1.25 eV according to v' = 8∿16.

Since general features of the vibrational transition cross sections $\sigma_{v_i \to v_f}$ are mostly determined by $\Delta v = v_f - v_i$, more specifically, $\sigma_{v_i \to v_f}$ and $\sigma_{v_i' \to v_f'}$ are in the same order of magnitude when $\Delta v = \Delta v'$ with $\Delta v' = v_f' - v_i'$, the strengths of the cross sections $\sigma_{0\to1}$ and $\sigma_{1\to2}$ will be quite similar to each other. For 2→3 transition, some peaks should appear at the threshold, since the v=3 vibrational energy level of O_2 coincides with that of v'=8 of the compound molecule O_2^-. However, this has not yet been confirmed by experiments.

REFERENCES

(1) Lane, N. F. and Geltman, S.: "Rotational Excitation of Diatomic Molecules by Slow Electrons: Application to H_2", Phys. Rev. 160, 53 (1967).

(2) Henry, R. J. W. and Lane, N. F.: "Polarization and Exchange Effects in Low-Energy Electron-H_2 Scattering", Phys. Rev. 183, 221 (1969).

(3) Lane, N. F. and Henry, R. J. W.: "Polarization Potential in Low-Energy Electron-H_2 Scattering", Phys. Rev. 173, 183 (1968).

(4) Hara, S.: "A Two-Center Approach in the Low Energy Electron-H_2 Scattering", J. Phys. Soc. Japan 27, 1009 (1969).

(5) Temkin, A. and Vasavada, K. V.: "Scattering of Electrons from H_2^+: The Method of Polarized Single-Center Orbitals", Phys. Rev. 160, 109 (1967).

(6) Temkin, A., Vasavada, K. V., Chang, E. S. and Silver, A.: "Scattering of Electrons from H_2^+. II", Phys. Rev. 186, 57 (1969).

(7) Temkin, A. and Faisal, F. H. M.: "Adiabatic Theory of Rotational Excitation of Non-Σ States", Phys. Rev. A3, 520 (1971).

(8) Chang, E. S. and Temkin, A.: "Rotational Excitation of Diatomic Molecules by Electron Impact", Phys. Rev. Lett. 23, 399 (1969).

(9) Henry, R. J. W. and Chang, E. S.: "Rotational-Vibrational Excitation of H_2 by Slow Electrons", Phys. Rev. A5, 276 (1972).

(10) Das, G. and Wahl, A. C.: "Extended Hartree-Fock Wave Functions: Optimized Valence Configurations for H_2 and Li_2, Optimized Double Configurations for F_2 ", J. Chem. Phys. 44, 87 (1966).

(11) Kolos, W. and Wolniewicz, L.: "Polarizability of the Hydrogen Molecule", J. Chem. Phys. 46, 1426 (1967).

(12) Hunter, G., Gray, B. F., and Pritchard, H. O.: "Born-Oppenheimer Separation for Three-Particle Systems. I. Theory", J. Chem. Phys. 45, 3806 (1966).

(13) Kolos, W. and Wolniewicz, L.: "Potential-Energy Curves for the $X^1\Sigma_g^+$, $b^3\Sigma_u^+$, and $C'\Pi_u$ States of the Hydrogen Molecule", J. Chem. Phys. 43, 2429 (1965).

(14) Choi, B. H. and Poe, R. T.: "Vibrational and Rotational Transitions in Low-Energy Electron-Diatomic-Molecule Collisions. II. Hybrid Theory and Close-Coupling Theory: An ℓ_z-Conserving Close-Coupling Approximation", Phys. Rev. A16, 1831 (1977).

(15) Hulbert, H. M. and Hirschfelder, J. O.: "Potential Energy Functions for Diatomic Molecules", J. Chem. Phys. 9, 61 (1941).

(16) Ehrhardt, H., Langhans, L. Linder, F., and Taylor, H. S.: "Resonance Scattering of Slow Electrons from H_2 and CO Angular Distributions", Phys. Rev. A17, 918 (1978).

(17) Linder, F. and Schmidt, H.: "Rotational and Vibrational Excitation of H_2 by Slow Electron Impact", Z. Naturforsch. 26a, 1603 (1971).

(18) Ehrhardt, H., Langhans, L., Linder, F., and Taylor, H. S.: "Resonance Scattering of Slow Electrons from H_2 and CO Angular Distributions", Phys. Rev. 173, 222 (1968).

(19) Burrow, P. D. and Schulz, G. J.: "Vibrational Excitation by Electron Impact Near Threshold in H_2, D_2, N_2 and CO", Phys. Rev. 187, 97 (1969).

(20) Linder, F. and Schmidt, H.: "Experimental Study of Low Energy e-O_2 Collision Processes", Z. Naturforsch. 26a. 1617 (1971).

*U.S.Government Printing Office: 1981 — 559-003/2008